General Disclaimer

One or more of the Following Statements may affect this Document

- This document has been reproduced from the best copy furnished by the organizational source. It is being released in the interest of making available as much information as possible.

- This document may contain data, which exceeds the sheet parameters. It was furnished in this condition by the organizational source and is the best copy available.

- This document may contain tone-on-tone or color graphs, charts and/or pictures, which have been reproduced in black and white.

- This document is paginated as submitted by the original source.

- Portions of this document are not fully legible due to the historical nature of some of the material. However, it is the best reproduction available from the original submission.

The Pennsylvania State University
The Graduate School
Department of Meteorology

REMOTE ESTIMATION OF SURFACE MOISTURE OVER A WATERSHED

A Thesis in
Meteorology
by
Paul Jeffrey Kocin

Submitted in Partial Fulfillment
of the Requirements
for the Degree of

Master of Science

November 1979

The Pennsylvania State University

The Graduate School

Department of Meteorology

Remote Estimation of Surface Moisture Over a Watershed

A Thesis in

Meteorology

by

Paul Jeffrey Kocin

Submitted in Partial Fulfillment
of the Requirements
for the Degree of

Master of Science

November 1979

The signatories below indicate that they have read and approved the thesis of Paul Jeffrey Kocin.

Date of Signature:	Signatories:
_____	_____ Toby N. Carlson, Associate Professor of Meteorology, Thesis Advisor
_____	_____ Hans A. Panofsky, Evan Pugh Professor of Atmospheric Sciences
_____	_____ Alfred K. Blackadar, Head of the Department of Meteorology

ABSTRACT

A numerical simulation of the ground temperature response is used in conjunction with satellite measurements of surface temperature to infer the moisture availability, a quantity which represents the amount of surface moisture. In addition to moisture availability, this numerical-graphical process derives evaporative and sensible heat fluxes at the surface; both of which are essential components in the surface energy budget.

Contoured analyses of moisture availability, moisture flux, sensible heat flux, thermal inertia, day and nighttime temperatures over a Missouri watershed are presented for two dates, one in June and one in September. Each field is discussed in terms of the region's surface characteristics (croplands, forests, creeks and small urban centers) and of rainfall accumulations. Forests and creeks exhibit the highest values of moisture availability whereas farmlands and villages are relatively dry.

The distribution of moisture availability over agricultural districts differs significantly between the two cases. This difference is attributed to a change in the surface's vegetative canopy between June and September, with higher moisture availabilities found in the latter case. Horizontal variations of moisture, however, do indicate some relationship between moisture availability and both local rainfall accumulations and the nature of the terrain.

TABLE OF CONTENTS

LIST OF FIGURES

LIST OF FIGURES (Continued)

ACKNOWLEDGEMENTS

I wish to express my sincere appreciation to Dr. Toby N. Carlson for his encouragement, guidance and patience during the preparation of this thesis. Similar appreciation is conveyed to Mr. Ralph Petersen and Mr. Locke Stuart of the NASA/Goddard Space Flight Center, for their efforts in providing data for this study. I am also grateful to James Cooper, Stan Benjamin and Joe Dodd for their programming assistance, and to my wife, Marla, whose editorial assistance and insights into organization proved invaluable.

The study was supported, in part, by the Environmental Protection Agency (EPA) under Contract R-805 G40020 and the National Aeronautical and Space Administration (NASA) Contract NAS-5-24264.

1.0 INTRODUCTION

1.1 The Need to Measure Surface Moisture

Water at the earth's surface is a natural resource whose abundance affects agriculture, hydrology and other vital human operations. Its global distribution has influenced the growth and destinies of civilizations and nourishes the many crops that feed the world's populations. According to Idso et al. (1975a), its presence in proper amounts is vital for all phases of crop growth: seed germination, early development and successful maturation. It is valuable to assess the amount of surface moisture in order to determine the apportioning of water intake from rainfall and irrigation into runoff, storage and deep percolation. With this information, hydrologists can estimate better the water balance of watersheds, and the likelihood of flooding events. To the meteorologist, surface water content is a necessary boundary condition for the determination of the surface heat flux in atmospheric models.

Idso and his colleagues commented that soil moisture influences crop productivity on a complex level. The water content of soil is the most basic ecological factor in the development of insects that spend all or a fraction of their lives in soil. Breeding and survival rates of larvae are influenced greatly by moisture content. Idso speculated that since it is impossible to watch over the breeding ground of many insect pests, the monitoring of surface wetness could be crucial in forecasting swarming dates in order to alert officials of the need for early pesticide applications before an outbreak becomes imminent. As an example, the desert locust, one of history's most serious agricultural problems, deposits its eggs just beneath the

ground surface. Development within the egg is entirely dependent on the absorption of water. This would necessitate the detection of changes in the surface water content in areas prone to this pest.

In addition to insect pests, Cook and Papendick (1971) have found that the growth and survival of plant pathogens is greatly dependent on the water content of the soil environment. The effect of water stress on pathogenic fungal growth is most important when soil is moist, as many forms of pathogens survive at various moisture levels. The moisture status not only directly affects the rate of disease activity, but it also influences disease activity indirectly through a variety of interactions.

The planting of crops could benefit by monitoring the surface water status because soil is often too dry for satisfactory seed germination. Bauer and his colleagues (1967) determined that soil moisture at seeding time is the best guide in determining nitrogen fertilizer needs of non-leguminous crops in studies done on farmland in the Northern Plains States.

Idso et al. (1975a) mentioned the effect of water content on pesticide residence times in soil. They speculated that a rapid assessment of a field's water content could alert farmers to the practicality of herbicide or pesticide application at a given time. Repeated measurements of ground moisture during the growing season could indicate whether the effects of pesticide application will carry over to the following season and whether these effects might interfere with the development of planned rotation crops.

Another use for monitoring soil moisture lies in erosion prediction. Wind erosion is a function of the cohesive forces of absorbed water

films surrounding soil particles. The loss of topsoil, due to the decrease in surface water content, may result in secondary effects such as air pollution by dust particles and abrasive action on other plants.

Finally, the study of landslides could benefit from the remote sensing of soil moisture. Blanchard et al. (1974) note that surface water increases weight, reduces shearing resistances and significantly reduces the shear strengths of minerals.

1.2 Background Work in Surface Moisture Measurements

Gravimetric measurements of soil water content, consisting of sectioning and weighing soil cores, followed by drying and reweighing, have been the standard method to ascertain a soil's moisture content. However, these measurements are laborious and applicable only to spatially small soil samples. Recently, the remote sensing of surface temperature has become a practical means of assessing the moisture status of the earth's heterogeneous fabric, which consists of cities, croplands, forests, etc. Extensive use of satellite, aircraft and instrumentation to measure the thermal, visible and microwave properties of the earth's surface, has enabled researchers to determine precisely the effective ground temperature and albedo. Estimates of surface moisture can thus be derived.

The associations between soil moisture content and temperature changes and gradients were demonstrated by Rose (1968), who compared water content with temperature profiles over a period of six days. Jackson (1973) reported that the liquid content of soil exhibits a marked diurnal variation with dehydration during the daylight hours

and partial rewetting at night. These variations are in response to the diurnal fluctuations of the many components of the surface energy budget, including solar, net and reflected radiation, wind speed, vapor pressure, air and soil temperatures, and soil water pressure-temperature-salt gradients. Jackson gravimetrically measured the water content of Adelanto loam concurrently with several of the aforementioned atmospheric variables, every half hour for two weeks, and found a water content maximum near sunrise and a minimum about two hours before sunset. He speculated that water content is dependent on temperature, with the amplitude of the moisture wave varying with season and depth.

Idso et al. (1975c) showed that albedo measurements could be used to delineate the three classical stages of soil drying, which are as follows: (1), the first stage is characterized by evaporation proceeding at the potential rate dictated by atmospheric conditions; (2), as the soil dries, hydraulic conductivity decreases to the extent that it can no longer supply water fast enough to meet atmospheric demand. Hence, the evaporation rate begins a faster decline from the rate of the previous stage; and (3), the evaporation rate levels out but at a very low rate that gradually approaches zero over a long period of time.

These three stages of soil drying were depicted by the daily variations of the soil's albedo, which was measured with simple solarimeters in an Arizona field of Avondale loam. When the albedo readings were correlated with gravimetrically measured values of soil water content, albedo was found to be a linear function of the water content of the soil surface. However, two major drawbacks prevent the

widespread application of this technique. First, the correlation between water content and albedo breaks down for small values of water content. Second, and probably more importantly, the albedos of different soils vary appreciably. Thus, there is little hope that a universal function will be worked out. Idso and his colleagues (1975b) used their finding that the albedo of wet soil is approximately half that of the same soil when dry, to develop a technique to calculate the daily rates of evaporation from wet and drying bare soils. This required additional knowledge of daily solar radiation and maximum and minimum air and surface temperature. Later, the same group (1977) extended their technique to include evaporation from vegetated and water surfaces.

Schmugge et al. (1974) demonstrated that emitted microwave radiation is a good indicator of soil water content over unvegetated terrain since the dielectric constant of water at microwave frequencies is frequently ten to twenty times that of dry soil. Varying the microwave frequencies produced differing but inconsistent results. However, the technique hinted at the possibility of extracting meaningful information without specifying the exact nature of the soil. Unfortunately, little further work was performed and problems arose, such as: (1), moisture induced emittance changes in soil that may not accurately reflect a correct variation in moisture content; (2), applicability is limited by a relatively coarse spatial resolution; and (3), salinity effects may alter microwave emissions.

A thermal inertia approach, in which the difference between maximum and minimum surface temperature is related to water content, was described by Myers and Heilman (1969). They found

that wet soils are generally cooler than dry soils during the day and vice versa at night. Idso and his associates (1975d) performed experiments on Avondale loam which indicated that the amplitude of the diurnal surface temperature wave could be used to yield satisfactory estimates of water content in the uppermost few centimeters of bare soil. In addition, Idso found a high correlation between water content and the difference between air and soil temperature, but the relationship again was dependent on soil type. Idso and his colleagues were interested in finding a continuous function which related thermal inertia to a soil water property independent of soil type. This led to their discovery of the relationship between water content and pressure potential (the tension with which water is held by soil particles). Pressure potential was found to be a linear function of water content for several soils tested. Investigations were made using pressure cells to measure the pressure potential over a range of 0 to -1 bar, with pressure membranes for the range of -2 to -15 bar, and by equilibration over salt solutions for the range of -15 to -6×10^6 bar. Pressure potential was found to be highly correlated with the diurnal surface soil temperature wave, yielding the possibility that a thermal inertia approach could be applied to determine a water content property for any soil.

A problem which arose with these applications was that of environmental variability: the non-uniformity from day to day, season to season, or from place to place of the external forcing functions of the daily surface temperature wave. Idso et al. (1976) noted that the diurnal surface temperature wave is a function of both internal and external factors. The internal factors: thermal conductivity,

density and heat capacity, define "thermal inertia". The external factors, including solar radiation, air temperature, etc., are expressed by the surface heat flux, which changes due to environmental variations in the external parameters. The change in the heat flux, in turn, alters the amplitude of the surface temperature wave. To compensate for this alteration, Idso utilizes National Weather Service air temperature measurements to normalize measured diurnal surface temperature variations to that of a "standard" air temperature variation.

Reginato et al. (1976) estimated moisture content for Avondale loam from thermal parameters previously discussed. However, they measured temperatures with thermocouples, portable infrared radiation thermometers located immediately above the ground, and aircraft multispectral scanners. Differences between maximum and minimum soil temperatures and maximum soil and air temperatures were correlated with moisture content from three samples of soil: (1), a wet section; (2), a dry section; and (3), an initially wet section that was allowed to dry. Results were similar to earlier studies but did not add substantially to the simplification of moisture measurements.

The subject of simple relationships between soil water content, an inherently difficult quantity to measure, and surface properties such as temperature change and albedo, which are much easier to measure, has shown to provide small improvements in the simplification of surface moisture measurements. At present, these studies are confined to limited soil types and spatial resolution, but hold promise for more widespread application.

Mathematical models, capable of simulating surface temperature and heat flux, have been employed in simulating the surface processes

which govern the atmospheric boundary layer. Carlson and Boland (1978) presented a method whereby surface temperatures, obtained remotely by an infrared radiometer, can be used in conjunction with a surface model to determine by graphical or numerical techniques, a measure of the surface moisture content. In this study, surface moisture is expressed as the moisture availability M; the fraction of maximum possible evaporation for a saturated surface. Thermal inertia, sensible heat flux, and evaporative fluxes are also determined by this method. The aim of their study was to analyze the substrate parameters and energy budget of urban areas, but the method has general applicability to other types of surfaces.

The concept of moisture availability M was introduced by Tanner and Pelton (1960) who utilized it in an energy balance approximation for estimating potential evapotranspiration. Use of this concept is necessitated by the fact that air in contact with the surface of the ground is not saturated, except where the land surface, itself, is saturated with water. Moisture availability is introduced to account for the reduction in the efficiency of evaporation due to subsaturation of the surface air. The factor M varies from zero for completely dry surfaces, to 1.0 for saturated terrain, such as soil surfaces following a substantial rainfall.

Nappo (1975) utilized the concept of moisture availability to parameterize expressions for the ground surface evaporative rate. He described the evaporation rate as a function of moisture availability and the difference between the saturation mixing ratio at the surface and that at the height of the lowest level in his model. Since M was difficult to measure, Nappo used a study by Davies and Allen (1973)

to evaluate this parameter. In their study, instruments determined the evaporation rate from two plots of rye grass on Fox loam. One plot was irrigated, the other was not. The measured evaporation rate from the irrigated field was set equal to the potential rate, while the rate from the non-irrigated field was set equal to the actual evaporation rate. The ratio of actual to potential evaporation rates defined the value of M. An expression for M related to water content was derived by examining gravimetric measurements of water content. However, this expression was applicable only for rye grass on Fox loam.

Boland (1977) expressed the evaporation rate as follows:

$$E_o = \rho \frac{L_e}{I} M \, (q_{os} - q_a) \qquad (1)$$

where ρ is the density of air, L_e, the Latent Heat of Vaporization. I, a resistance function, is essentially the vertical integral of the inverse of molecular and eddy diffusivities, q_{os} is the surface saturation mixing ratio and q_a, the mixing ratio at the top of the surface layer. Carlson and Boland (1978) used this expression to represent the evaporative flux in their model, but developed a technique which determines M as part of an iterative solution to a boundary layer model rather than prescribing it from substrate characteristics, an impractical task for a large domain.

Dodd (1979) examined the spatial distribution of moisture availability, as well as thermal inertia, surface heat flux and evaporative flux over the Los Angeles and St. Louis regions for May 30-31 and June 9-10, 1978, respectively. Using Carlson and

Boland's method, he demonstrated the marked effect that reduced evaporation has in producing the urban "heat island". He found that urban areas possess maxima of surface heat flux and minima of surface moisture flux while forests and grassy areas display the opposite trend. Values of M ranged from less than 0.2 over urban centers to greater than 0.9 over forested regions.

1.3 Purpose of Thesis

Moisture measurements have been limited to specific soil types and small soil samples. These restricted studies have severely limited the applicability of such measurements. This research examines the distribution of moisture availability on a relatively large spatial scale: specifically over a watershed region large enough to include croplands, forests, creek beds and villages. A model inversion method developed by Carlson and Boland (1978) is used in conjunction with satellite measurements to infer surface moisture, whereby moisture availability and thermal inertia are varied systematically in a one dimensional boundary layer model to simulate the temperature response at the ground. Temperatures simulated in the model corresponding to those satellite measurement times are then matched with satellite-derived radiometric temperatures to arrive at a solution for M, as well as thermal inertia and the surface heat and evaporation fluxes.

Although soil moisture itself is not directly measured, moisture availability describes the water content of any surface, whether it be soil, cropland or an agglomerate of urban structures. It can be considered an approximate measure of the average fractional saturation

of the ground surface. In addition to measuring moisture availability, heat and evaporative fluxes, which determine the temperature response of the surface to radiational forcing, are evaluated. This method also allows one to analyze the surface energy budget over a watershed region.

The Goodwater Creek Watershed and surrounding areas in central Missouri (Figure 1) is chosen as the working area because of its agricultural makeup and potential value as a watershed research site. The derived patterns of moisture availability, thermal inertia, heat and evaporative fluxes from two cases, one from the late spring, the other from early autumn, are first described in terms of the character of the surface canopy. Second, differences in these quantities between the two cases are related to atmospheric variables and rainfall amounts.

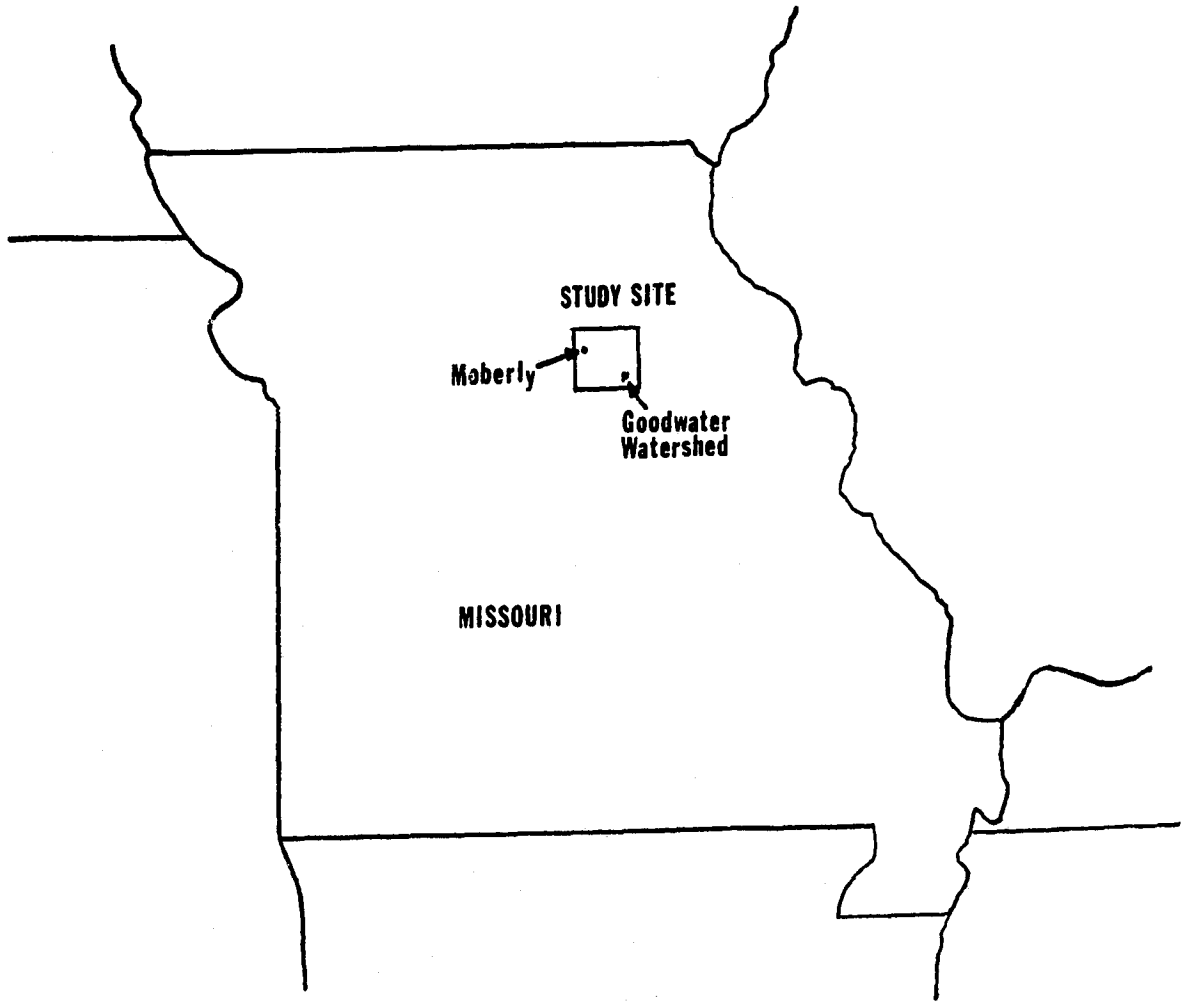

Figure 1. Location of Goodwater Watershed and surrounding countryside.

2.0 METHOD OF ANALYSIS

Carlson and Boland's technique to infer the moisture availability and thermal inertia is documented thoroughly by Boland (1977) and by Dodd (1979). This method is briefly described in this section.

A one-dimensional boundary layer model was developed to calculate: (1), temperature profiles in the atmospheric surface layer (50 meters) and in the top meter of the underlying soil layer; and (2), fluxes of sensible heat and moisture at the earth's surface over a diurnal cycle. The temperatures obtained from the model are matched against observed temperatures by a series of regression equations relating moisture availability, thermal inertia, sensible heat and evaporative flux to the temperatures at the times of satellite measurements.

The model was created on the premise that the diurnal temperature fluctuation close to the surface responds to radiative forcing, the character of the underlying substrate, and the turbulent nature of the surface layer wind field. Large scale considerations such as advection are ignored due to their complexity. K-type parameterizations for eddy fluxes are utilized. Two features included in the model are: (1), the concept of a near surface transition layer of height Z_{ℓ} located above an effective radiating surface, within which molecular, radiative and turbulent mechanisms co-exist to convey heat upwards or downwards; and (2), the inclusion of a daytime mixed layer which is modified at night to permit the downward transfer of heat through the stable region below, in order to balance radiative losses at the surface.

The basic framework of the model consisting of a substrate layer, a transition layer near the ground surface, a turbulent air layer and a mixing layer, is displayed in Figure 2. Wind speed u_a, temperature T_a, and specific humidity q_a at the top of the surface layer (Z_a = 50 meters), roughness length and the temperature at the base of the substrate slab (1.5 meters below the surface) are initially prescribed. The time dependent diffusion equation is integrated to predict soil layer temperature changes. The temperature and moisture distributions in the surface layer are determined by a succession of equilibrium states ascertained from a solution of the surface energy balance which is constrained by similarity theory in the atmosphere and the diffusion equation in the soil.

The primary forcing in the model is the net radiation

$$R_N = G_o + H_o + E_o \tag{2}$$

where G_o, H_o and E_o are, respectively, the heat flux into the ground, the sensible heat flux and the latent heat flux into the atmosphere. The net radiation is represented by the difference between: a), the sums of the solar flux absorbed at the ground and downward terrestrial flux; and b), the upward terrestrial flux. Details of the radiation model are given by Augustine (1978). The surface heat flux, H_o, is parameterized in terms of an eddy diffusivity, K_H, a molecular diffusivity, C_s, and a vertical potential temperature gradient, $\frac{\partial \theta}{\partial z}$. The water vapor flux, E_o, is parameterized in terms of an eddy and molecular diffusivity for water vapor and a vertical mixing ratio gradient. As described in section 1.2, this flux may

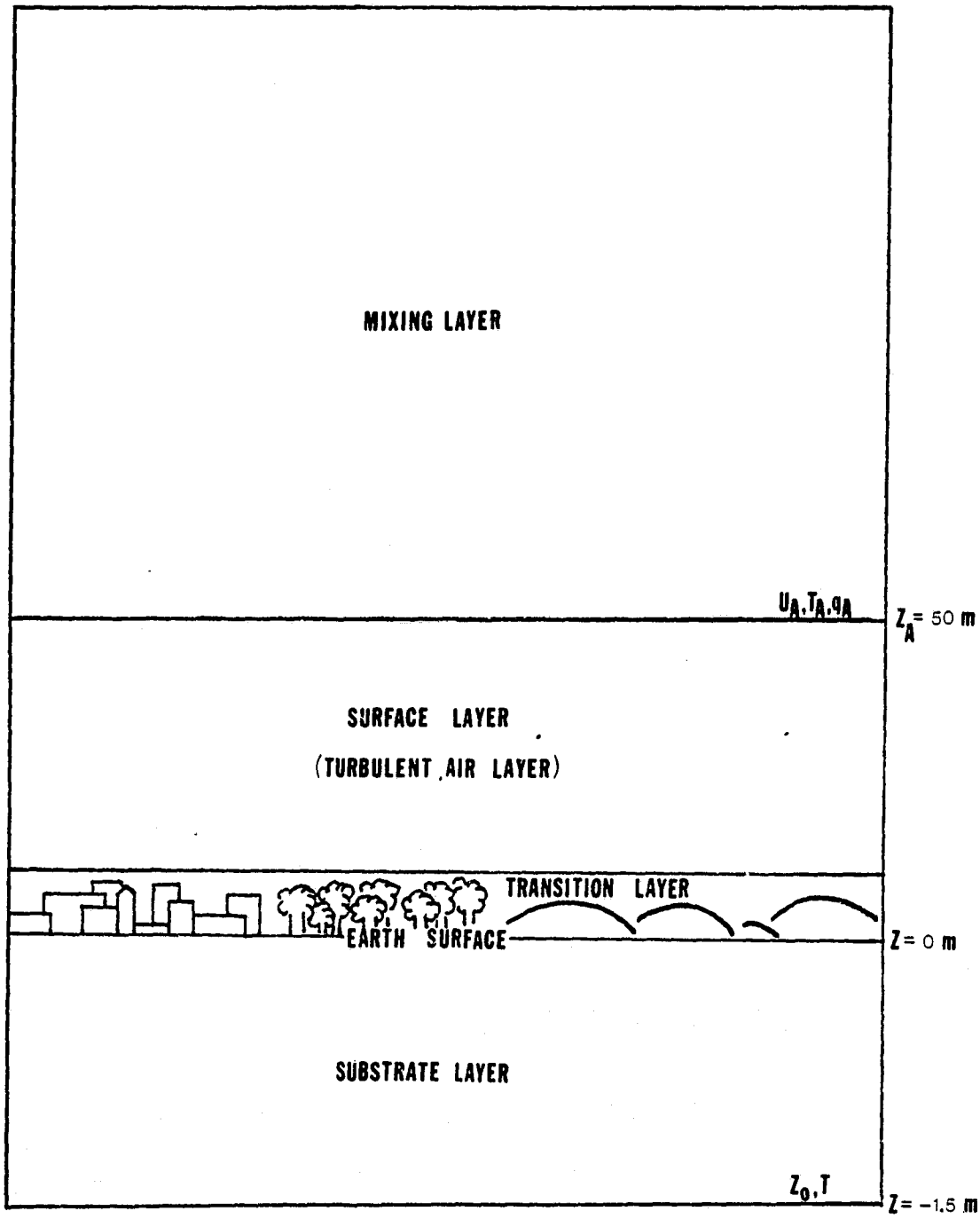

Figure 2. Basic framework of model.

also be expressed in terms of the moisture availability M. Ground heat flux, G_o, is given as a function of soil thermal conductivity and the temperature gradient immediately below the soil-air interface. The transfer of heat through the soil is governed by the diffusion equation where the thermal inertia P, here defined as

$$P = (C_g \lambda_s)^{1/2} = \lambda_s \kappa_s^{-1/2} \tag{3}$$

represents the substrate heat storage ability. C_g represents the ground heat capacity, λ_s, the thermal conductivity of the substrate, and κ_s, the thermal diffusivity of the substrate.

During the day, the surface temperature and mixing ratio are derived by integrating expressions for the sensible heat flux and evaporative flux. In essence, this integration is performed in two vertical sections: (1), from the effective surface to the height of the surface transition layer, where molecular and radiative heat transfer mechanisms become small; and (2), from that height to the top of the surface layer, where Monin-Obukhov scaling is applicable.

An equation for the sensible heat flux at the surface, combining expressions for ground heat flux, evaporative flux, potential temperature and the energy balance, is derived and cycled through for convergence. Net radiation, friction velocity, a flux integral of the inverse of molecular and eddy diffusivities, heat flux, surface temperature and evaporative fluxes are calculated. Convergence is achieved when successive iterations of four minutes per time step through the cycle result in small changes in heat flux or friction velocity between cycles. Once convergence is attained,

ground heat flux and sub-surface heat transfer are calculated over four substrate levels by integration of the diffusion equation.

A mixed layer formulation developed by Tennekes (1973), was used to correct for the underestimation of the amplitudes and phase lag of the temperature beyond solar noon, the time of maximum heating. This formulation allows the temperature at the top of the surface layer (T_a) to be adjusted by raising the height of the mixed layer during the day. As the height of the mixed layer rises, air from above with a higher potential temperature (θ) is brought downward; hence, θ is raised in the mixed layer and T_a is altered. A similar correction for water vapor enables the mixing ratio at the top of the surface layer to vary with time.

At night, the upward heat flux vanishes and radiational cooling permits surface temperatures to decrease with time. Subsequently, the heat flux becomes dependent on the temperature lapse rate near the ground. A scheme proposed by Blackadar (1976) has been modified and incorporated into the model, whereby the turbulent exchange of momentum at night is calculated as a function of the Bulk Richardson Number B in the surface layer. When the Bulk Richardson Number becomes greater than 0.2, the decrease of ground temperature and wind shear stress acts to decouple the surface layer from the above atmosphere. In turn, the wind above the surface will accelerate, increasing the shear. If this shear becomes large enough to allow B to fall below 0.2, a turbulent, downwardly directed exchange of heat occurs, which elevates the surface temperature for a time. Numerical tests conducted by Dodd (1979) and by Blackadar[1] indicate that this

---

[1]Private communication.

formulation is likely to correctly predict the nights that experience turbulent episodes but not the exact times of the episodes themselves.

Model output must be used in conjunction with measured values of temperature. The NASA Heat Capacity Mapping Mission (HCMM) satellite is able to provide .6 km resolution measurements of radiometric ground temperature over a large and heterogeneous surface, such as that of a watershed region. HCMM is a polar orbiting satellite which has the capability of taking measurements over a site twelve hours apart. An important feature of this satellite is its orbital schedule which allows measurements to be made close to times of maximum and minimum surface temperatures; approximately 2 p.m. and 2 a.m. local time, respectively.

Radiometric data of the earth's surface called digital count or DN values, are taken from raw data tapes obtained from NASA and copied onto a standard labelled tape, from which smaller regions can be extracted and analyzed. The digital count information can be converted to alphanumeric characters, each representing a range of temperatures. This information is represented as a character map in which individual pixels corresponding to geographic locations are assigned reference coordinates. The digital values are equated to temperature using a calibration equation for HCMM data, which has a temperature range of 260° to 340° K representing count values of 0 to 255. The effective surface temperature maps are then depicted in a variety of ways using computer graphics, plotters and color enhancement.

Satellite temperature measurements are used in conjunction with the model results to determine maps of moisture availability M, thermal inertia P, and the surface heat fluxes H_o and E_o.

Typically, the model is initialized at a time near sunrise and allowed to proceed for a day or more. Initial values of wind speed, temperature and moisture are obtained from local soundings and representative values of albedo, roughness and turbidity are included in the model. After each cycle, the model is reinitialized with incremented values of M and P until 16 cycles are completed over the maximum likely range for M(.05 - 1.0) and P(.005 - 0.1). A graphical representation of the solutions for the relationship between M, P and surface temperature is illustrated in Figure 3. In this diagram, a pair of M and P values within their full range of physically realistic values corresponds to a unique solution for a given pair of observed day and night temperatures. These solutions are represented by the intersections of the day temperature curves versus M and P (running top left to bottom right) and night temperature curves (running top right to bottom left).

At two specified times during each of the 16 cycles, corresponding to times of day and night satellite passes, the model results are extracted, stored and subsequently used to determine a set of model output regression equations between predicted temperatures, the surface fluxes and the parameters M and P. For a parameter X representing M, P, or surface fluxes, a second order regression equation is fitted with the form

$$X = C_1 + C_2T_D + C_3T_D^2 + C_4T_N + C_5T_N^2 \qquad (4)$$

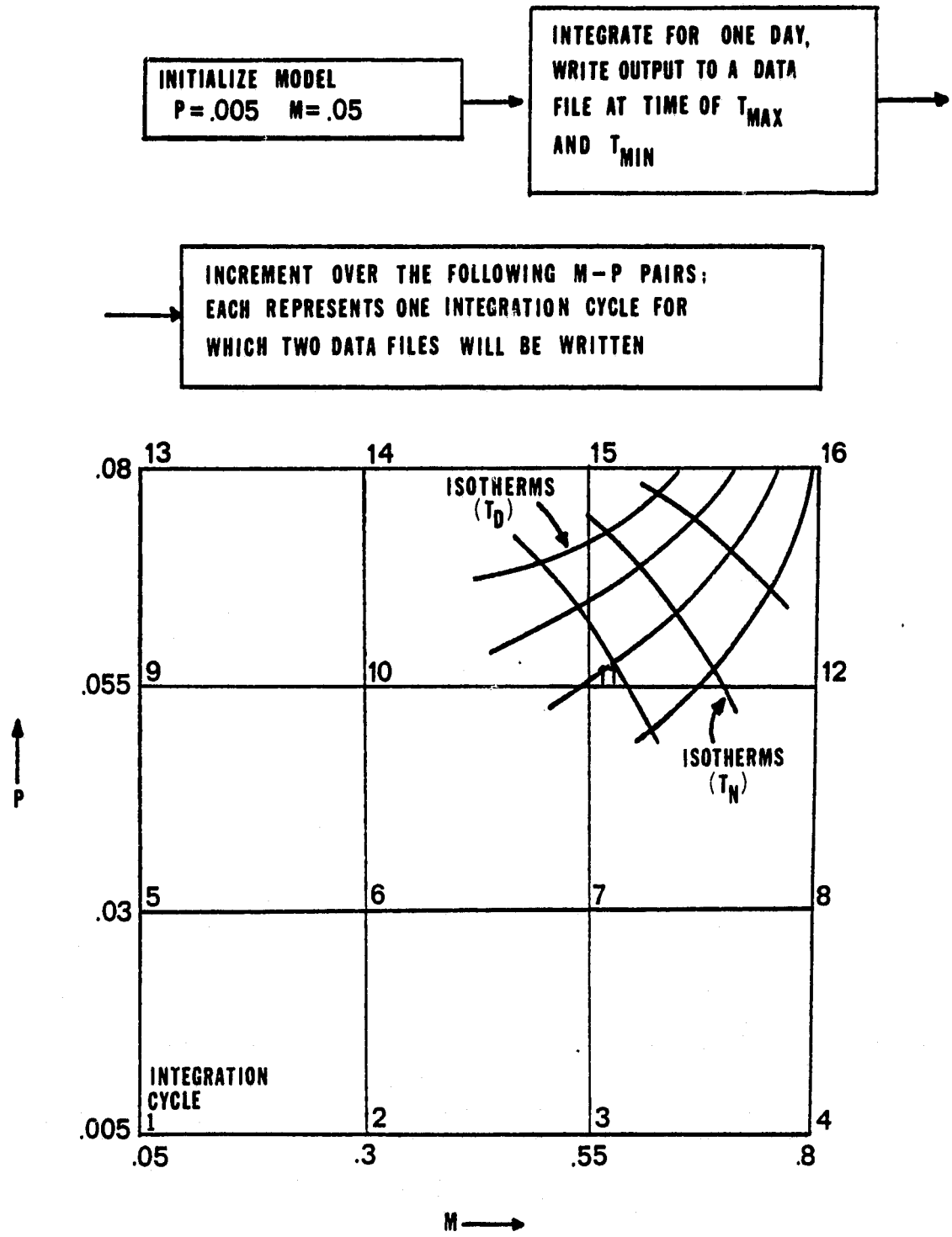

Figure 3. Schematic illustration of incrementation process and day/night temperature arrays.

where the coefficients C_1 - C_5 are determined from the 16 sets of model results for the daytime and nighttime temperatures, T_D, and T_N, respectively.

Model results indicate that M, P and the fluxes vary monatonically and almost linearly with T_D and T_N over almost the entire range of values, the exceptions being at extreme values of M or P where, in any case, there is very little variation of X with temperature. Thus, except for isolated occasions with extreme values of M or P, the solutions are single valued.

The last step in the analysis procedure is to transform the rectified temperature images contained in a two-dimensional array to maps of M, P, H_o and E_o. This is done by inserting the measured temperatures into the regression equations determined from the model output. Maps of these parameters are then contoured and displayed.

3.0 RESULTS

3.1 Regional Description

Figure 4 presents a base map of the Missouri agricultural region, upon which analyses of moisture availability, moisture flux, sensible heat flux, thermal inertia, daytime temperatures and nighttime temperatures are displayed. The dashed area located in the lower right hand side of the figure corresponds to the boundary of the Goodwater Watershed defined by the U.S. Department of Agriculture in Centralia. The agricultural site covers approximately 1600 km^2: forested regions are colored dark grey while bare soil and low vegetation appear lightly shaded. The following locations are coded for easy identification:

SCL - Sugar Creek Lake

M - Moberly

PC - Perche Creek

EC - Elk Creek

CC - Coon Creek

HC - Hardin Creek

MC - Milligan Creek

SC - Saling Creek

S - Substation

SF - Silver Fork

C - Centralia

GC - Goodwater Creek

LBC - Long Branch Creek

BC - Bee Creek

SR - Salt River

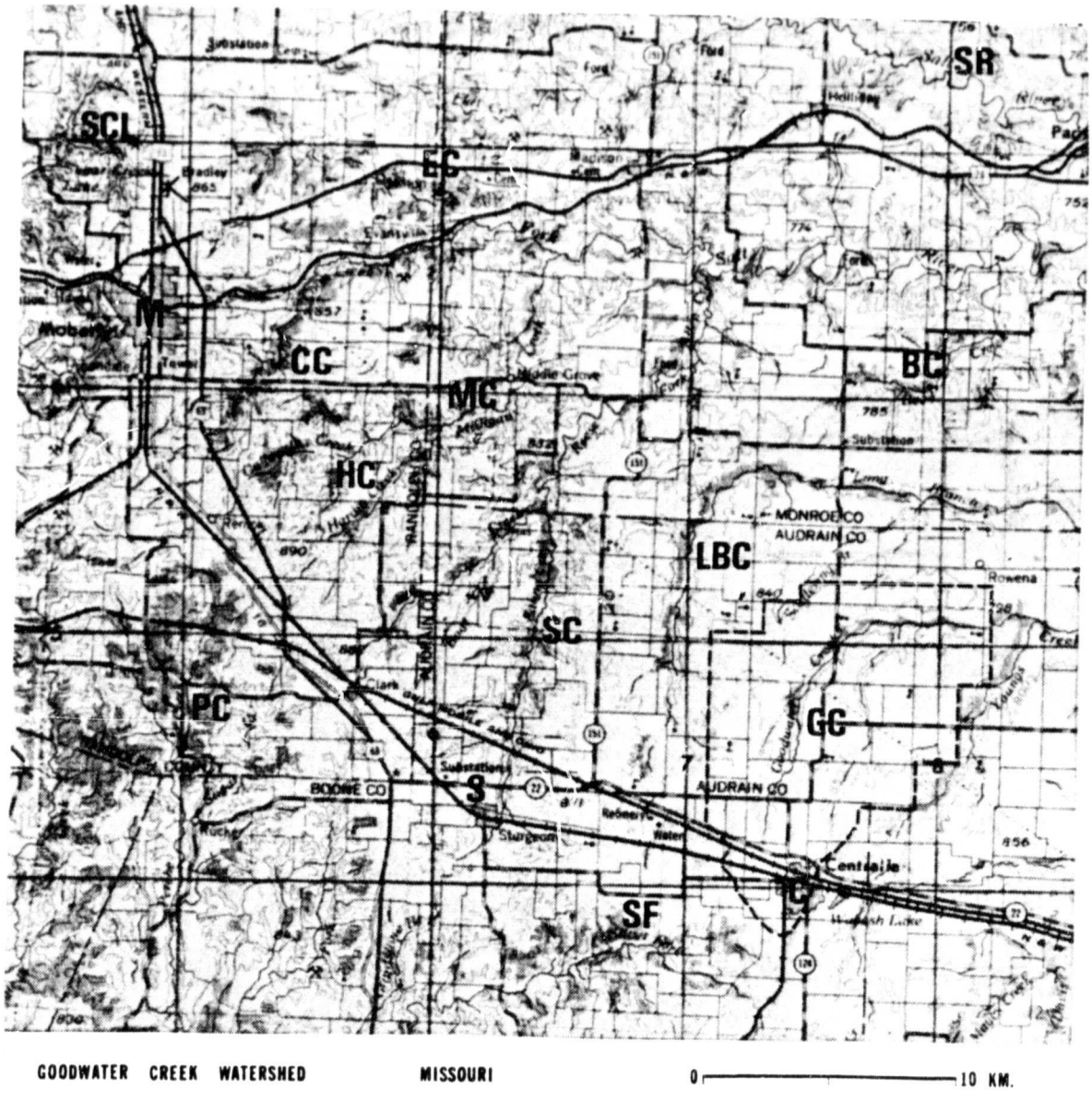

Figure 4. Base map of the Missouri Agricultural site with a letter key marking areas of interest referenced in text

The area is characterized by gently rolling hills with much cropland. Land use surveys show that approximately eighty five percent of the region around Centralia is cultivated, three quarters of which consists of corn, wheat, soybeans, milo sorghum and several varieties of hay. Small grain, legumes and grasses cover the remainder of the cultivated land. The remaining fifteen percent of the region is uncultivated, composed mainly of pasture, timber and small urban centers. The largest villages, Moberly and Centralia, have populations of 12000 and 5000, respectively.

3.2 Background

An ideal study of moisture availability measurements should include at least two cases from approximately the same time of year to eliminate any seasonal variations in the surface water content. Ideally, one of the dates should follow an extended period of dryness, while the other date should follow a substantial rainfall. A study such as this allows an easy evaluation of moisture availability variations due to changes in rainfall.

However, a day/night pair of temperatures derived from HCMM data for a specific location on earth can be accessed only once every sixteen days, due to the satellite's orbital characteristics. Given consistent cloudless conditions, we are presented with a maximum of twenty three days year round for potential analyses. Since skies are rarely cloud-free, only a few dates are available for research. The satellite Tiros-N offers more frequent data, but its coarser spatial resolution removes much of the detail necessary for this type of study.

The two cases examined in this study, June 9-10, 1978 and September 29, 1978, were chosen for three reasons: (1), both cases occurred at times of the year when temperatures are relatively similar; (2), clear skies predominated, allowing unobstructed measurements of surface temperature; and (3), temperature advection was small, so that the assumptions within the model were not violated.

The satellite images for the June case pertain to data thirty-six hours apart: the night pass occurring at approximately 2 a.m. on June 9 and the day pass at 2 p.m. on June 10. The model is initialized at 6 a.m. from June 9 meteorological data and allowed to cycle for thirty-six hours, in order to simulate afternoon temperatures the next day. The model includes a variable surface initialization to account for a slight warming trend on June 10.

It is assumed that the surface temperature wave is essentially stationary for both June 9 and June 10. Therefore, the model output derived from June 9 initial conditions is actually for 2 a.m. and 2 p.m., June 10, the former occurring twenty-four hours after its corresponding satellite orbit time. This artificial reversal of orbit times in the model will not substantially affect the final results.

The satellite images for the September case were taken twelve hours apart. However, the nighttime images were taken at 2 a.m. September 29, twelve hours before, rather than thirty-six hours following the daylight orbit (as in the June case). Similarly, stationarity is assumed in the temperature response in order to justify a reversal in the ordering of the day/night sequence in the model, the night orbit being presumed to have occurred at 2 a.m. on the 30th.

3.3 Missouri Agricultural Site, June 9-10, 1978

Figures 5 and 6 present the observed day and night ground temperatures for June 10 and June 9, 1978, respectively. Figures 7, 10, 11 and 12 present the fields of moisture availability, sensible heat flux, evaporative flux and thermal inertia derived by Carlson and Boland's technique.

Clear skies and unseasonably cool temperatures, as a result of a large ridge of high pressure traversing the state of Missouri, dominated the weather during this period. Early morning air temperatures were observed to be generally between eight and twelve degrees Celsius. Afternoon temperatures on the tenth were generally between twenty-two and twenty-seven degrees Celsius. Precipitation that had occurred as recently as June 6-7 amounted to a few tenths of an inch.

During the two weeks prior to this period, rainfall amounted generally to an inch or less, leading to speculation that moisture content at the time of the study would be relatively low.

3.3.1 June 10 Daytime Temperatures

Daytime surface temperatures, shown in Figure 5, range from less than 23°C to 29°C. Crop and pasture land, consisting of open fields of low vegetation, exhibit the highest temperatures, ranging generally between 26°C and an isolated 29°C, three kilometers northeast of Moberly (M). The warmest zone extends from the northwest sector of the map southward through Moberly, then southeastward to Substation (S). Other agricultural lands with temperatures greater than 27.5°C are denoted by W's.

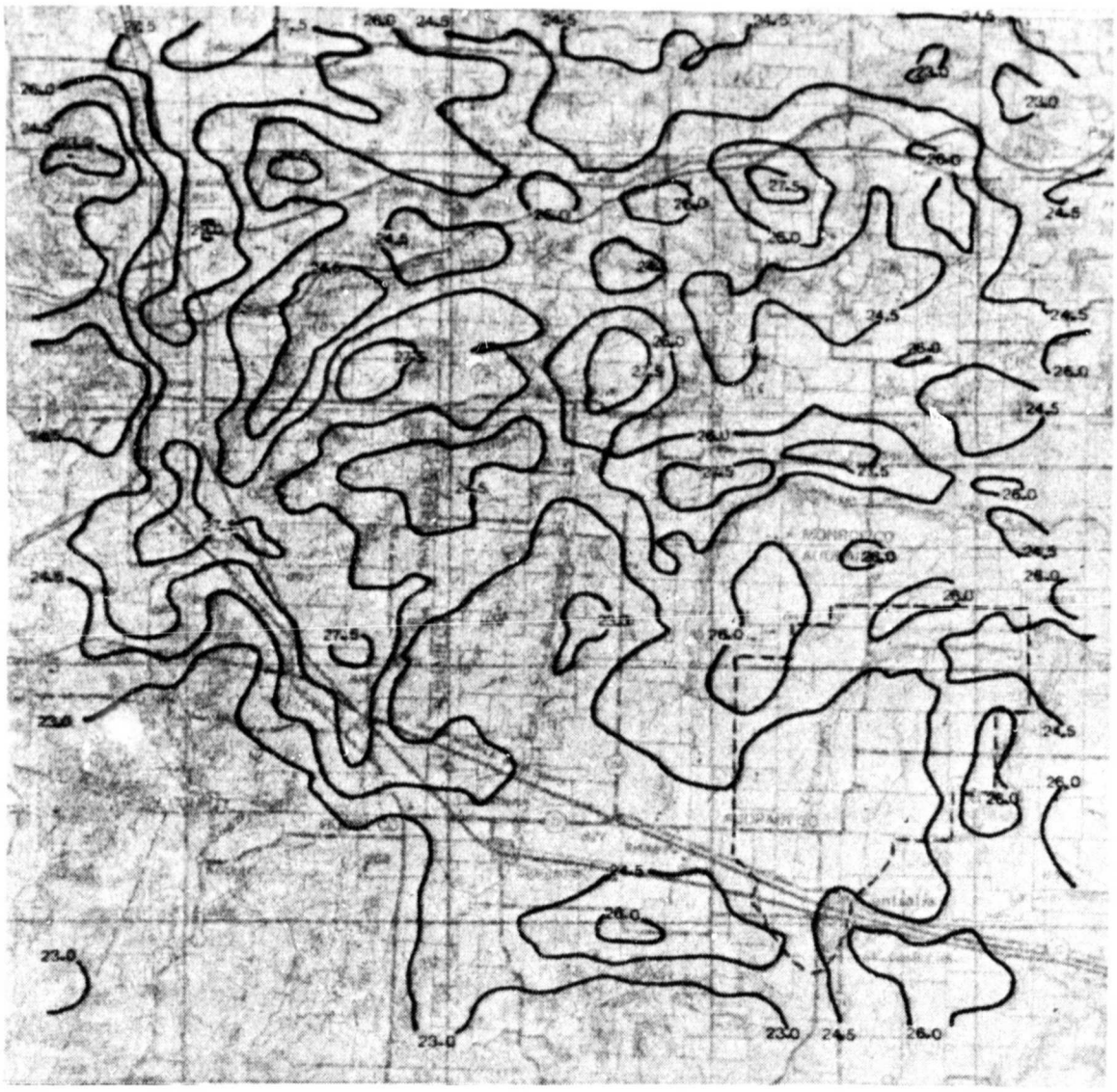

Figure 5. Daytime surface temperature analysis (°C) at approx. 2:00 p.m. June 10, 1978

Moberly and Centralia appear as temperature maxima relative to their surroundings. However, temperatures are seen to decrease sharply toward the west from the western half of Moberly. A probable explanation for this temperature decrease is a heavily forested area immediately to the west of Moberly. The decrease across Moberly itself is due to smoothing within the graphics program, resulting in the temperature gradient being spread over a larger area.

Forest lands and river beds appear associated with surface temperatures of 24.5°C or less. Lowest temperatures (23.0°C or less) are found along or near Sugar Creek Lake (SCL), Perche Creek (PC), Silver Fork (SF), and the Salt River (SR). Temperatures between 23.0°C and 24.5°C can be found along the Elk (EC), Coon (CC), Hardin (HC), Milligan (MC), Saling (SC) and Bee Creeks (BC) and a forest immediately to the west of Moberly. Contrary to expectation, relatively warm temperatures (approx. 27.5°C) are found along Long Branch Creek (LBC). The creek may have run dry, exposing a rapidly heated rocky basin.

Within the (dashed) Goodwater Watershed, temperatures are generally less than 24.5°C, but no specific surface features can be identified by the temperature pattern with the exception of Centralia, which appears as a relative temperature maximum.

3.3.2 June 9 Nighttime Temperatures

The nighttime isotherm pattern, Figure 6, exhibits a smaller temperature range than the daytime pattern, from 3.5°C to 6.5°C, while most temperatures fall between 4.0 and 5.5°C.

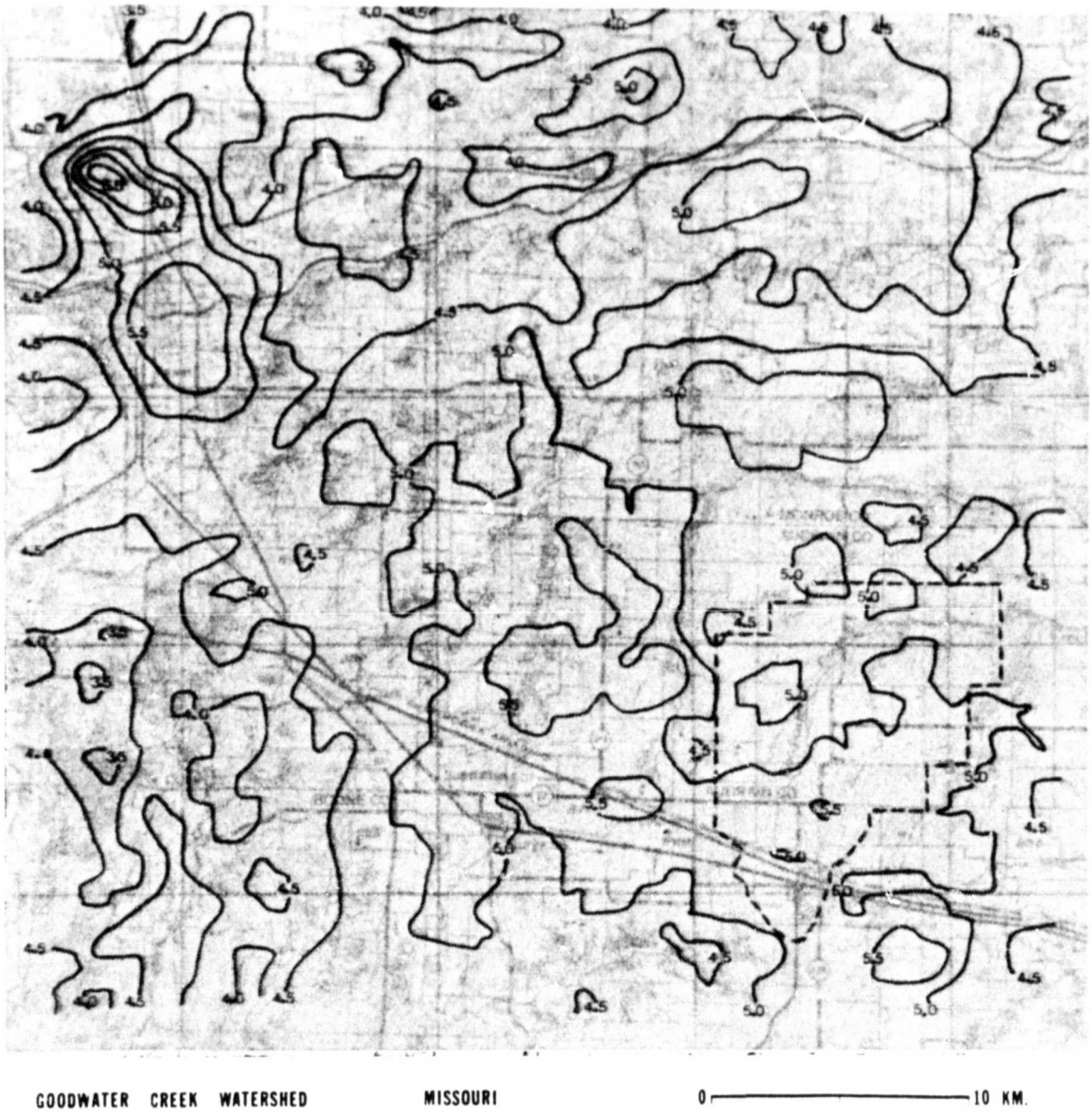

Figure 6. Nighttime surface temperature analysis (°C) at approx. 2:00 a.m. June 10, 1978

The simple one-to-one correspondence between land use and temperature, clearly illustrated by the daytime temperature configuration, is lost at night. The only distinct thermal patterns appear near Sugar Creek Lake, where a maximum temperature occurs because Sugar Creek Lake is the largest body of water within the figure. The model is essentially invalid over deep water which has a nearly infinite storage capacity for solar radiation.

Unfortunately, few other temperature features correspond to specific land usage. Moberly appears as a relative maximum of temperature (5.5°C), while Centralia does not, owing to its small size. Temperatures greater than 5°C are found throughout the central and southeastern sectors.

Forest regions, situated west of Moberly and in the southwestern corner of the figure near Perche Creek, appear as temperature minima. The (dashed) Goodwater Watershed exhibits a temperature range of 4.5°C to 5.5°C.

3.3.3 June 9-10 Moisture Availability, M

Moisture availability values (Figure 7) vary from just under .40 to greater than .90. The pattern of M reveals a striking inverse correlation with daytime temperature; small values of M are highly correlated with daytime maximum temperatures and vice versa. Thus, a dry surface suppresses evaporation, allowing a greater partitioning of the net radiation into sensible heat flux, thereby yielding greater surface heating. A moist surface partitions more energy into latent, rather than sensible heat flux, resulting in suppressed heating. M values greater than .90 are found in forested areas surrounding Perche Creek. Much of the southwest quadrant of

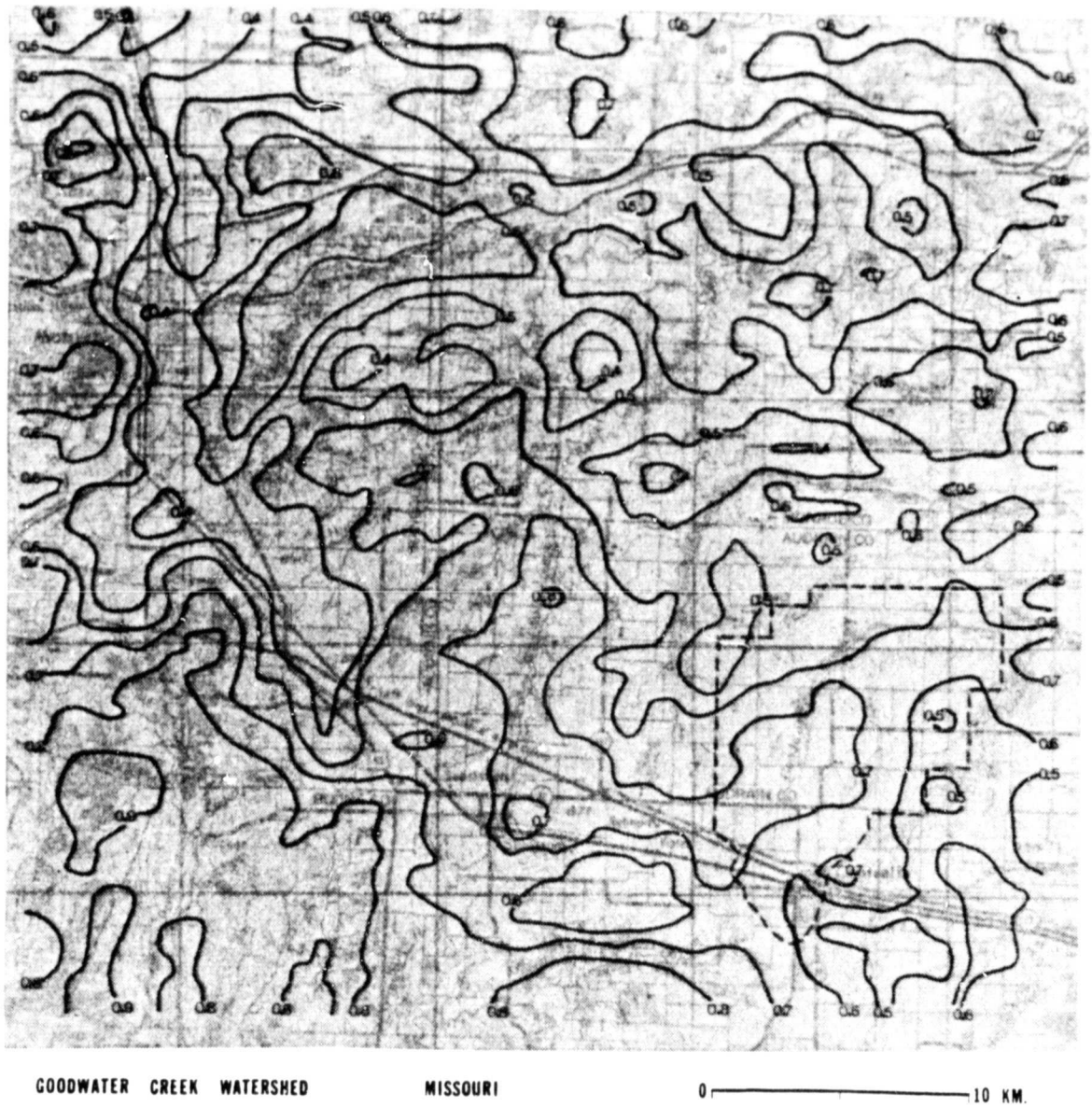

Figure 7. Moisture availability analysis, June 10, 1978

Figure 7 displays moisture availability measurements exceeding .80, a value which appears valid for forest canopies where transpiration is an important component of the energy balance. Over Sugar Creek Lake and Saling Creek, M is found to be greater than .80 owing to the area's predominant mixture of forests and lush vegetation.

A small spatial change from forest to agricultural land results in a large gradient of M. This is particularly evident ten kilometers south of Moberly, where smoothing techniques within the analysis program eliminate the sharpness of the moisture discontinuity along the boundary. The most prominent moisture availability minima (.40-.50) are located just east of Moberly along agricultural lands extending north-south for approximately twenty five kilometers.

Relative minima in Moberly and Centralia undoubtedly result from alteration of the surface energy budget due to urbanization. Moberly's moisture availability is less than that over Centralia due to the larger size of Moberly. Minima of M (less than .50) are found scattered throughout the farming areas and possibly, near dry creeks.

High values of M (greater than .70) are found along the many creeks that run through the region. Generally M ranges from .60 to 1.0 for forest and river districts, and from .35 to .60 for agricultural locations.

Figure 8 presents an enlarged and finely detailed analysis of moisture availability over the Goodwater Watershed (enclosed by dashed lines) and adjacent areas. The added detail results from plotting the raw data without smoothing and highlights the moisture features more accurately.

Figure 8. Enlargement of unsmoothed moisture availability analysis over the Goodwater Watershed (enclosed by dashed lines), June 10, 1978

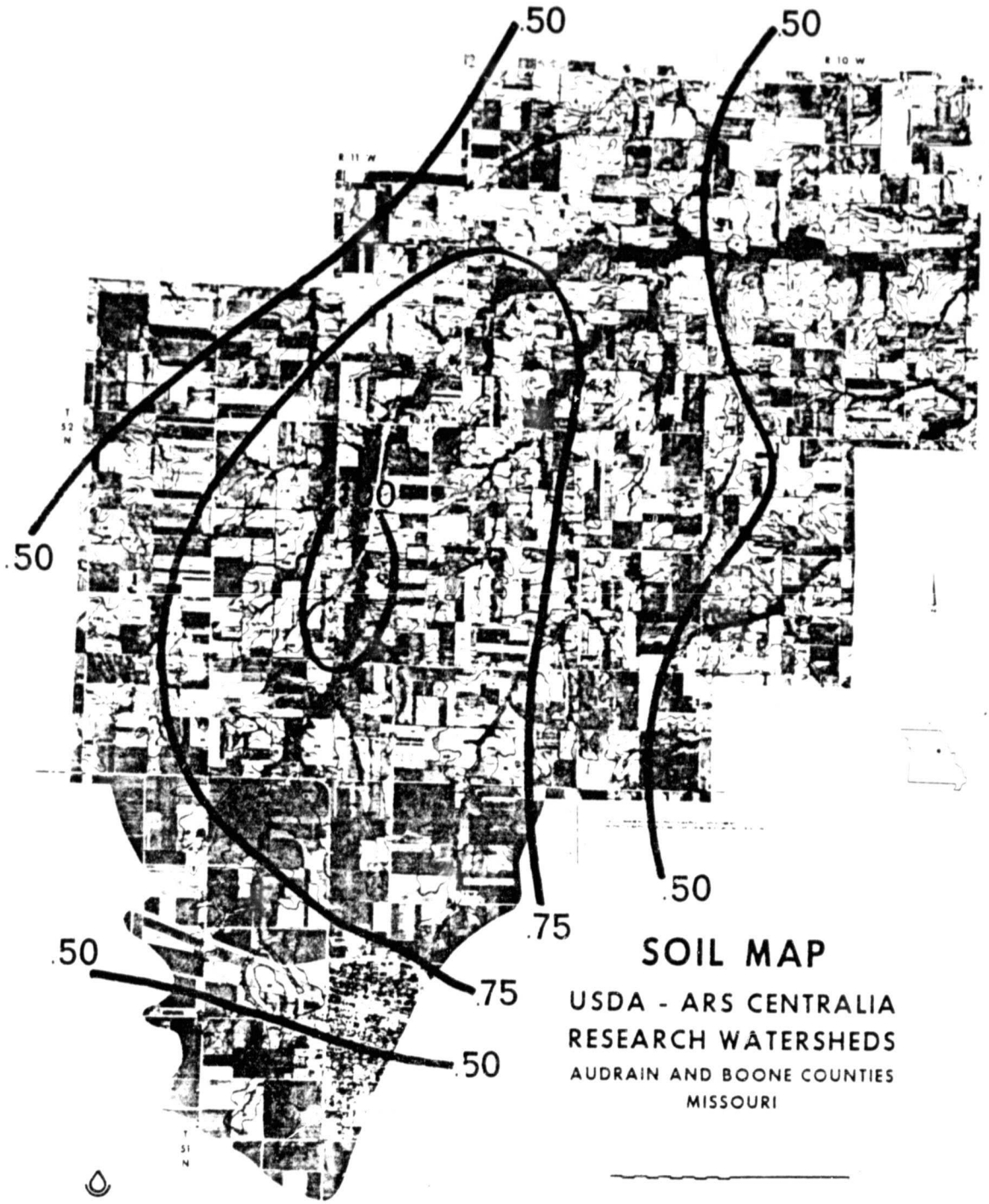

Figure 9. Rainfall amounts (in inches) over the Goodwater Watershed, June 1, 1978 - June 7, 1978

A large variation of M can be noted over the Goodwater Watershed, with a minimum of .40 over Centralia and a maximum of .80 over Goodwater Creek. In this analysis, agricultural districts are now represented by a relatively large variation of M values; from less than .50 to greater than .75. Long Branch Creek is represented as an M minimum (M less than .50), implying that either the creek has dried out along the section running north-south, or that it has little vegetation. Over the east-west section of the creek, M ranges from .60 to .80. Saling Creek, at the left edge of the figure, is represented by values of M between .70 and .90. Forested sites surrounding Silver Fork, at the bottom of the figure, are represented by M values between .80 and 1.0.

Rainfall totals between June 1, 1978 and June 7, 1978 for the Goodwater Watershed are shown in Figure 9. The analyses are derived from daily observations from 16 stations within the watershed. An aerial photo of the watershed is used as the map base. Heaviest rainfall, greater than three quarters of an inch, occurred throughout the central section of the watershed, while less than one half inch fell in the south, the extreme northwest, and the northeast.

Highest values of M (greater than .70) are found over regions having had the heaviest rainfall, while low values of moisture availability (less than .60) are found in areas of small rainfall accumulations.

3.3.4 June 10 Surface Heat Flux, H_o

The analysis of the surface heat flux, (Figure 10) was determined for the early afternoon of June 10. The contour pattern closely resembles the daytime temperature pattern: high values of heat flux

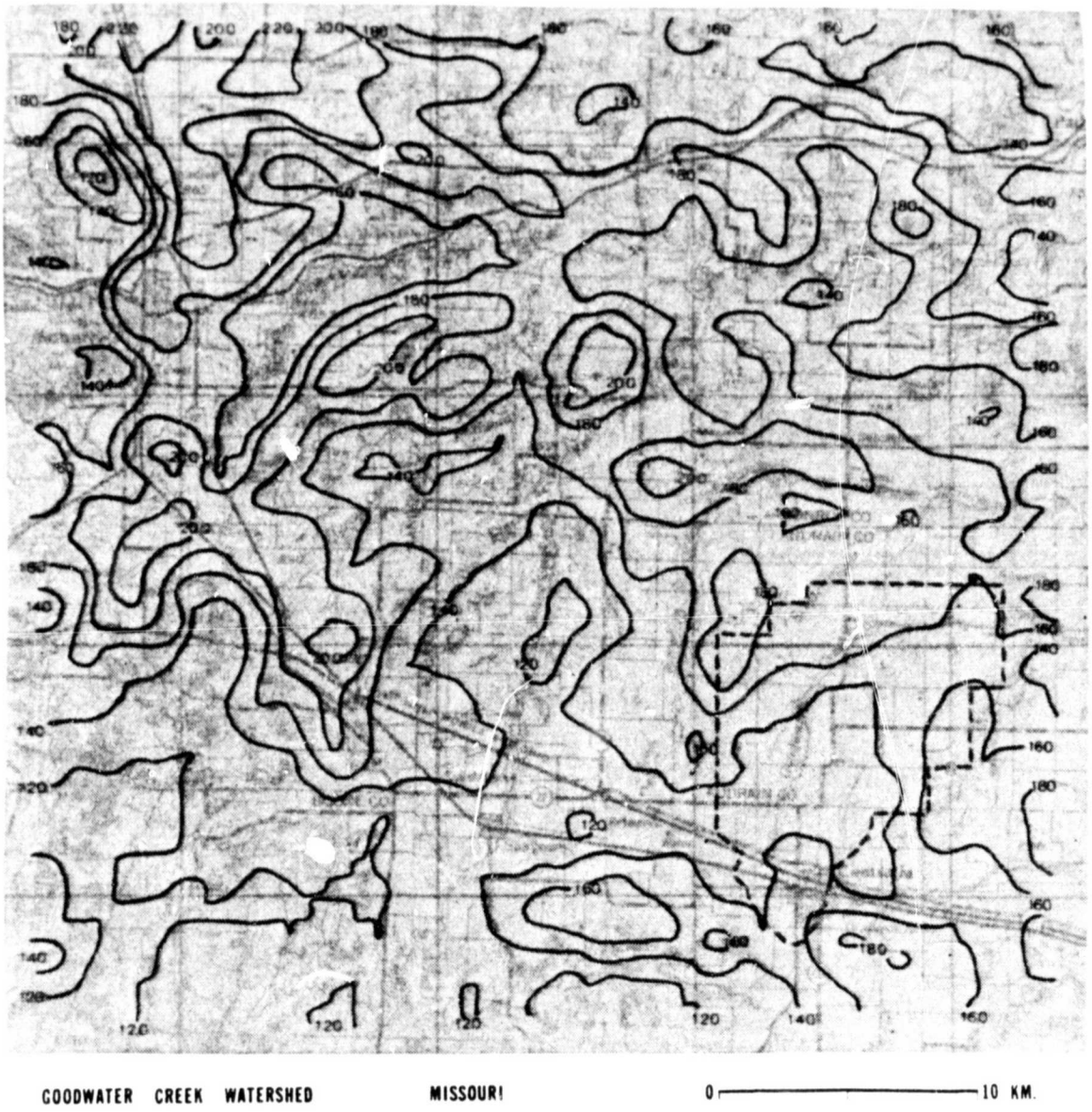

Figure 10. Sensible heat flux (Wm^{-2}) at approx. 2:00 p.m., June 10, 1978 (R_N = 650 Wm^{-2})

correspond to high amplitudes of temperature; the same holds true for small magnitudes of heat flux and temperature. Values of heat flux range from 120 to 220 Wm^{-2}. Lowest values are found over Sugar Creek Lake, south of Silver Fork, along Saling Creek and surrounding Perche Creek. These heat flux minima correspond geographically to daytime temperature minima. Both features are found over a surface composed of deciduous canopies and creeks, where the apportioning of net radiation into latent heat predominates. Typical sensible heat fluxes 140 Wm^{-2} or less are found in these locations.

Moberly is seen as a heat flux maximum (180 Wm^{-2}) due to the alteration of the energy budget as a result of urbanization. Centralia is poorly defined as a relative maximum of heat flux. Highest values are found over crop and pasture land on a north-south line running from northeast of Moberly to Substation (S). A maximum reading of 220 Wm^{-2} can be seen about ten kilometers northeast of Moberly. Small agricultural regions exhibiting isopleths of heat flux greater than 200 Wm^{-2} are scattered five to ten kilometers north of the center of the figure. Dodd (1979) examined the heat flux pattern for the same day over the St. Louis region. He found very similar results, but over downtown St. Louis, values were as high as 250 Wm^{-2}.

3.3.5 June 10 Evaporative Flux, E_o

Isopleths of surface evaporative flux, shown in Figure 11, vary from approximately 360 Wm^{-2} to 530 Wm^{-2}. Distributions of high values of moisture flux correspond roughly to areas of low heat flux, and vice versa. Minimum values of evaporative flux (360 Wm^{-2} to 400 Wm^{-2}), are found over the same regions where heat flux is

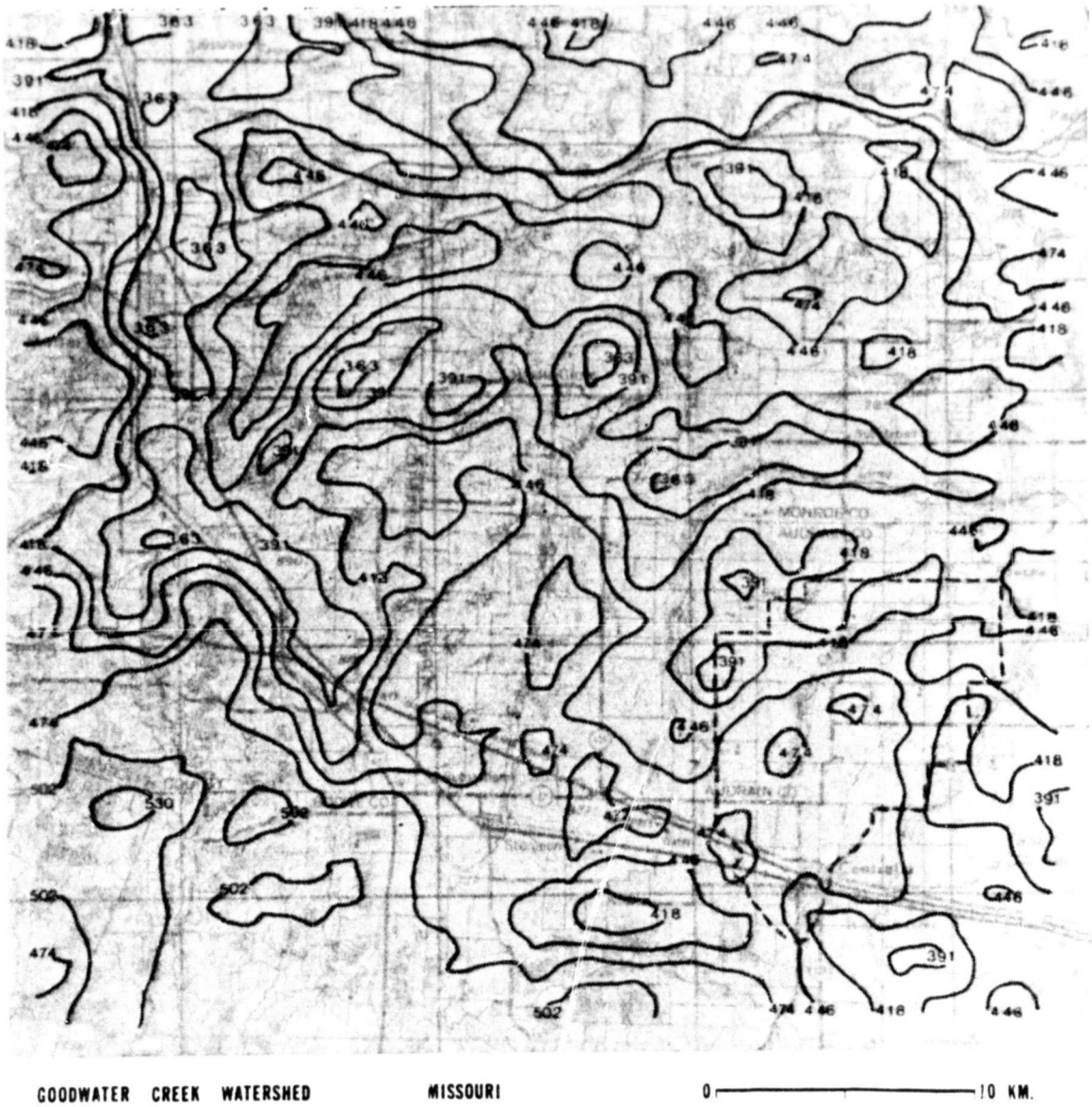

Figure 11. Evaporative flux (Wm^{-2}) at approx. 2:00 p.m., June 10, 1978 (R_N = 650 Wm^{-2})

measured at 180 Wm^{-2} or higher. The evaporative flux was largest over a heavily forested region near Perche Creek. High moisture fluxes are noted over forests, since moisture that is normally lost to the ground is absorbed through the roots of trees and subsequently transpired.

Most agricultural regions, including the (dashed) Goodwater Watershed District, have a flux range of 360 Wm^{-2} to 440 Wm^{-2}. Goodwater Creek, showing up as a minimum of heat flux, here appears as a maximum of evaporative flux. The northwest corner of the area shows up as a relative maximum of heat flux and a minimum of evaporative flux. Largest fluxes are observed over forests, lakes and creeks, while lowest values can be found over farmland and urban centers.

3.3.6 June 9-10, Thermal Inertia, P

The distribution of thermal inertia P, Figure 12, is relatively unremarkable, exhibiting a range almost exclusively between .03 and .04. In his study of the St. Louis region, Dodd (1979) reported a variation between .03 and .05, similar to the range of values derived in this study. Generally, those areas with large diurnal temperature changes have small values of thermal inertia, while the converse also holds true. The only distinct variation of thermal inertia is located at Sugar Creek Lake, where P is greater than .045, due to the exceptionally large heat storage ability of water surfaces. However, over bodies of water, the analyses are spurious.

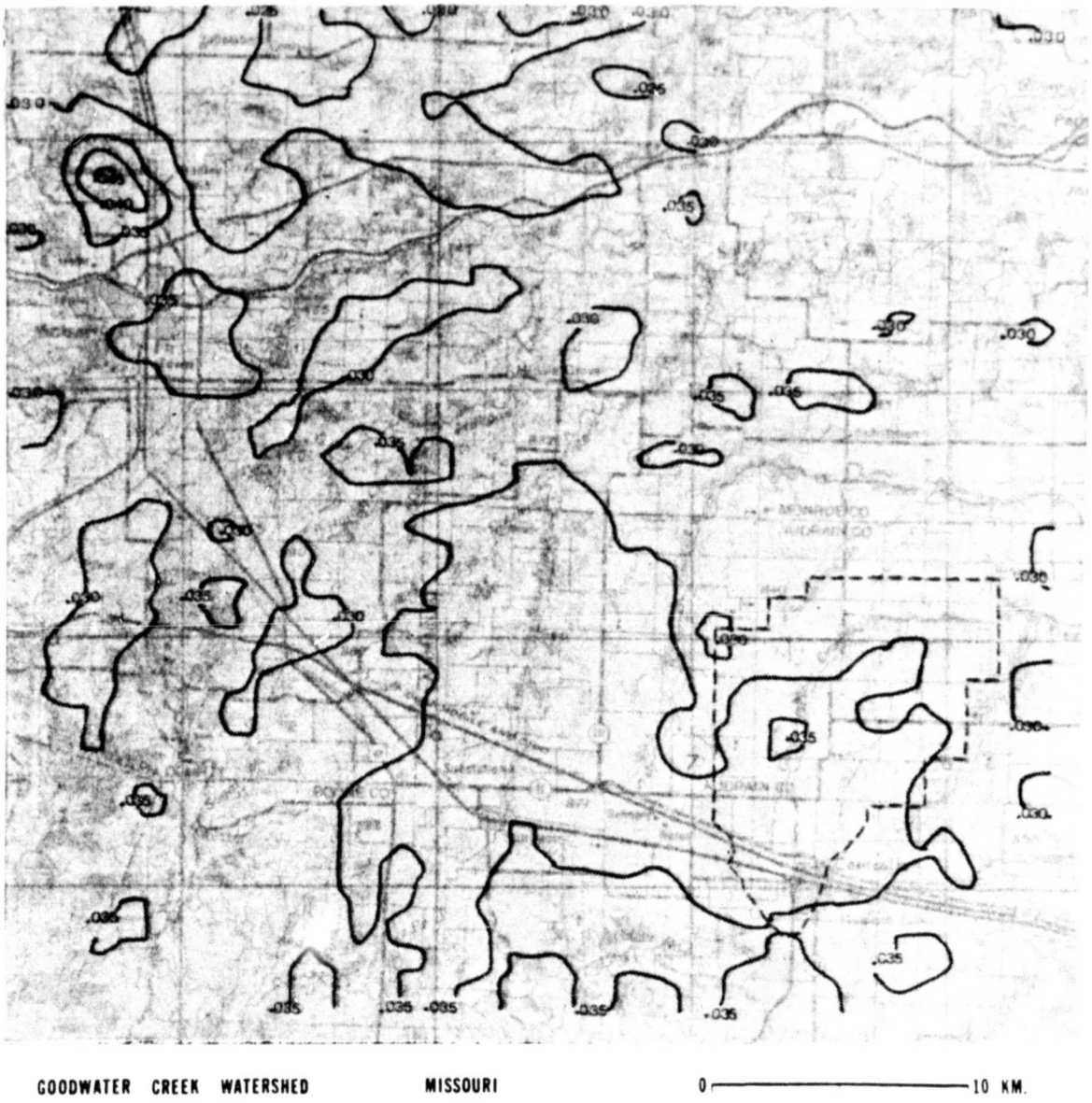

Figure 12. Thermal inertia analysis (cal cm^{-1} K^{-1} $sec^{-1/2}$), June 10, 1978

3.4 Missouri Agricultural Site, September 29, 1978

Measured day and nighttime surface temperatures for September 29, 1978 are presented in Figures 13 and 14. Contoured analyses of moisture availability, sensible heat flux, evaporative flux and thermal inertia are presented in Figures 15, 18, 19 and 20.

A ridge of high pressure, centered to the east of Missouri on the morning of the twenty ninth, provided clear skies and relatively calm winds. A frontal system advancing from the Plains States preceded a slight warming trend during the afternoon hours. However, this trend did not become established until a few hours after the p.m. satellite temperature measurements were made. Morning air temperatures varied generally between six and ten degrees Celsius, while early afternoon values were near or slightly above twenty degrees Celsius.

The interposition of a small cloud on the southwest portion of the area during the time of the afternoon orbit resulted in an erroneous determination of moisture availability, sensible heat flux, evaporative flux, and thermal inertia over the extreme southwestern top of the working area. This area will be neglected in subsequent discussions.

The last recorded rainfall prior to the case study occurred on September 20, averaging approximately one half inch. Through the twenty-ninth, September rainfall totals were proportionately light, averaging around two inches.

3.4.1 September 29 Daytime Temperatures

The daytime surface temperature map, presented in Figure 13, exhibits a range of values from just below 20°C to 24°C. Despite

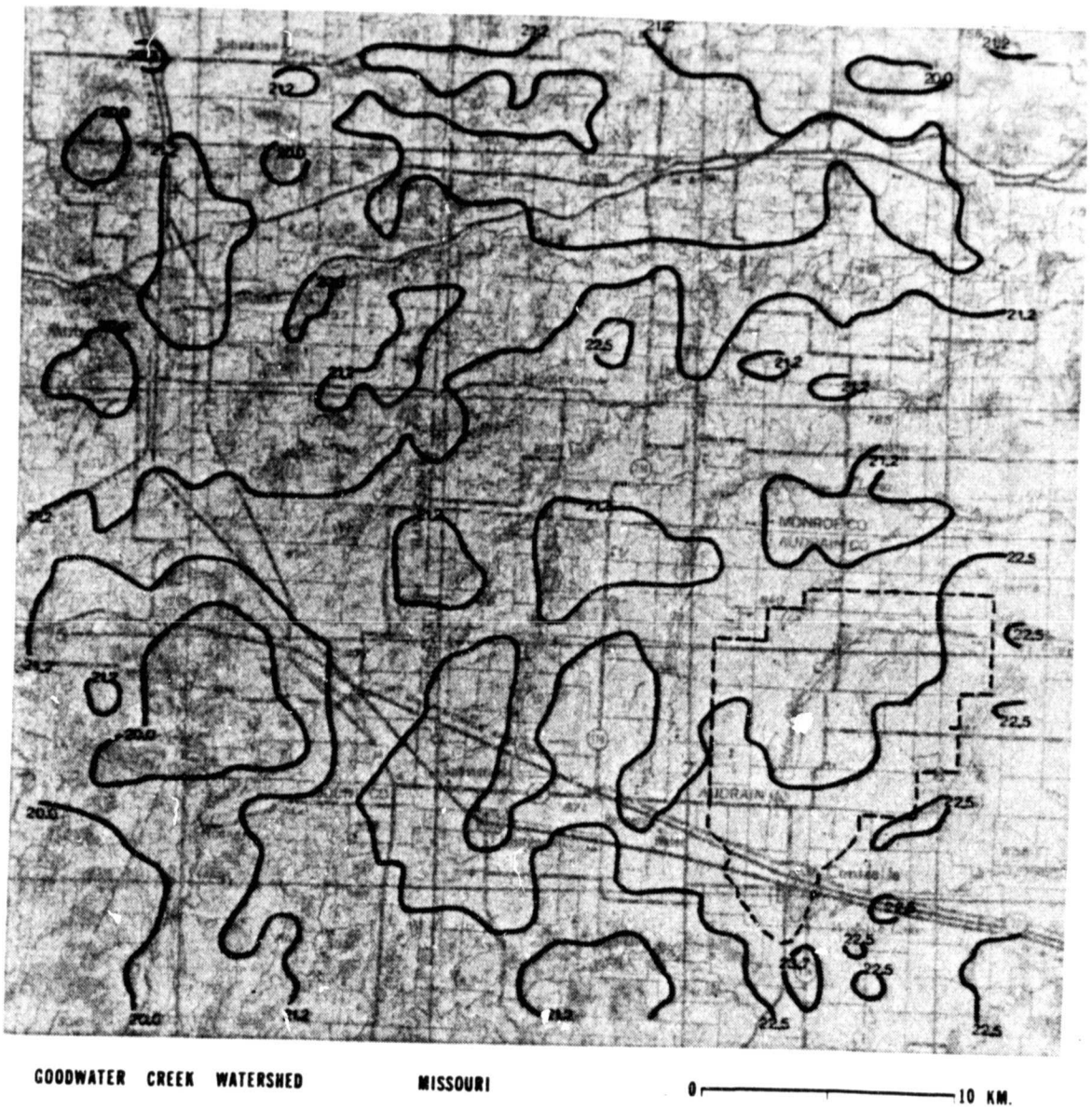

Figure 13. Daytime surface temperature analysis (°C) at approx. 2:00 p.m. September 29, 1978

small temperature variations between crop, forest, watershed and village, subtle differences in land usage can be detected from the figure.

Highest temperatures (greater than 22.5°C) are located throughout the southeastern quadrant of the figure. These regions, in addition to other sections with slightly lower temperatures, are characterized by extensive fields of vegetation. A region of maximum temperature (23.7°C) is found immediately south of Centralia. Whereas both Centralia and Moberly were readily identifiable in the June 10 isotherm pattern, on September 29, only Moberly is distinguishable as a slight thermal maximum.

Lowest temperatures (20°C or less) are located approximately where low temperatures were recorded on the afternoon of June 9. Forests dominate these regions and include the areas surrounding Perche Creek, Moberly and Sugar Creek Lake.

Land temperatures appear only slightly warmer than water surfaces. The temperature over Sugar Creek Lake is only one to two degrees Celsius lower than the surrounding land. On June 10th, the lake's surface temperature was measured as much as six degrees Celsius lower than nearby land surfaces.

In general, warmest surface temperatures are located in the map's southeastern sector while lowest temperatures are found along the western boundary. Small elevations in temperature of approximately one degree Celsius can be observed along several creeks, including Silver Fork, Saling Creek, Long Branch Creek and Salt River. Within the (dashed) Goodwater Watershed region, temperatures range from 21°C to 23°C; lowest values are found in the north and highest values in the south.

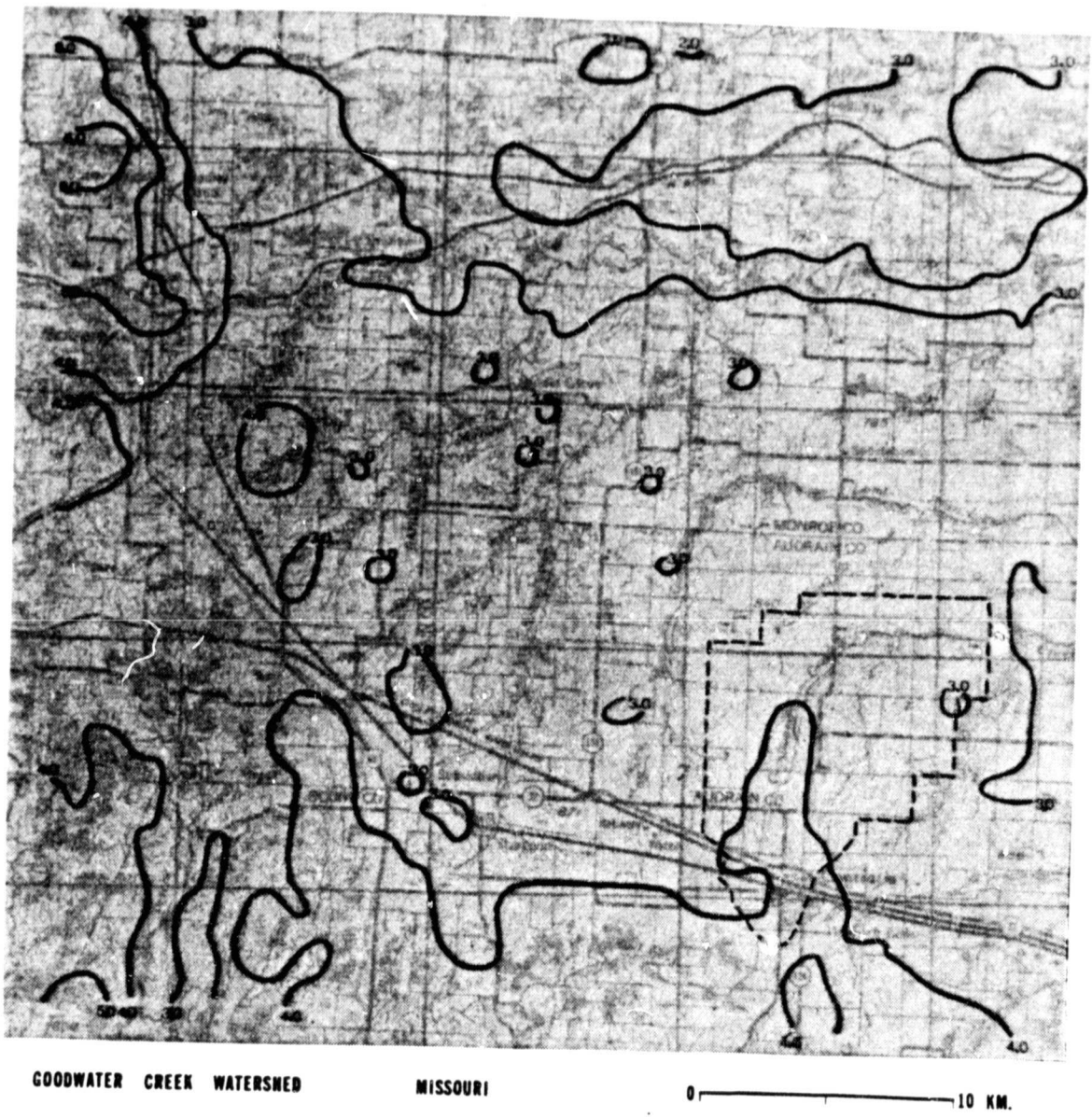

Figure 14. Nighttime surface temperature analysis (°C) at approx. 2:00 a.m. September 29, 1978

3.4.2 September 29 Nighttime Temperatures

The analysis of nighttime surface temperatures, Figure 14, depicts a larger range of temperatures than was observed the morning of June 9th. Temperatures vary primarily between 2.5°C and 4.5°C, but values as low as 2°C and as high as 6°C can be noted. Sugar Creek Lake, the warmest feature on the morning of June 9, again appears as the major temperature maximum (greater than 6.0°C). Its relatively high temperature is primarily due to the storage of solar energy.

Agricultural lands appear as relative temperature minima (between 2°C and 4°C) while forested sites are noted as relative temperature maxima (greater than 4°C). Both Moberly and Centralia appear within contours of proportionately high temperature. Over the (dashed) Goodwater Watershed, temperatures vary from 3°C to 4°C, with a narrow tongue of temperatures greater than 4°C extending northward from Centralia.

Both day and nighttime thermal patterns show a small latitudinal temperature gradient, with colder temperatures to the north. This gradient was not apparent in the June case study.

3.4.3 September 29, Moisture Availability, M

The analysis of moisture availability, Figure 15, shows neither the large range of M values nor the large spatial gradients of M that characterized the June case study. Despite the lack of measureable rainfall for over a week preceding the satellite measurements, moisture availability values are uniformly high, varying primarily from .60 to 1.0; however, the majority of values fall somewhere between

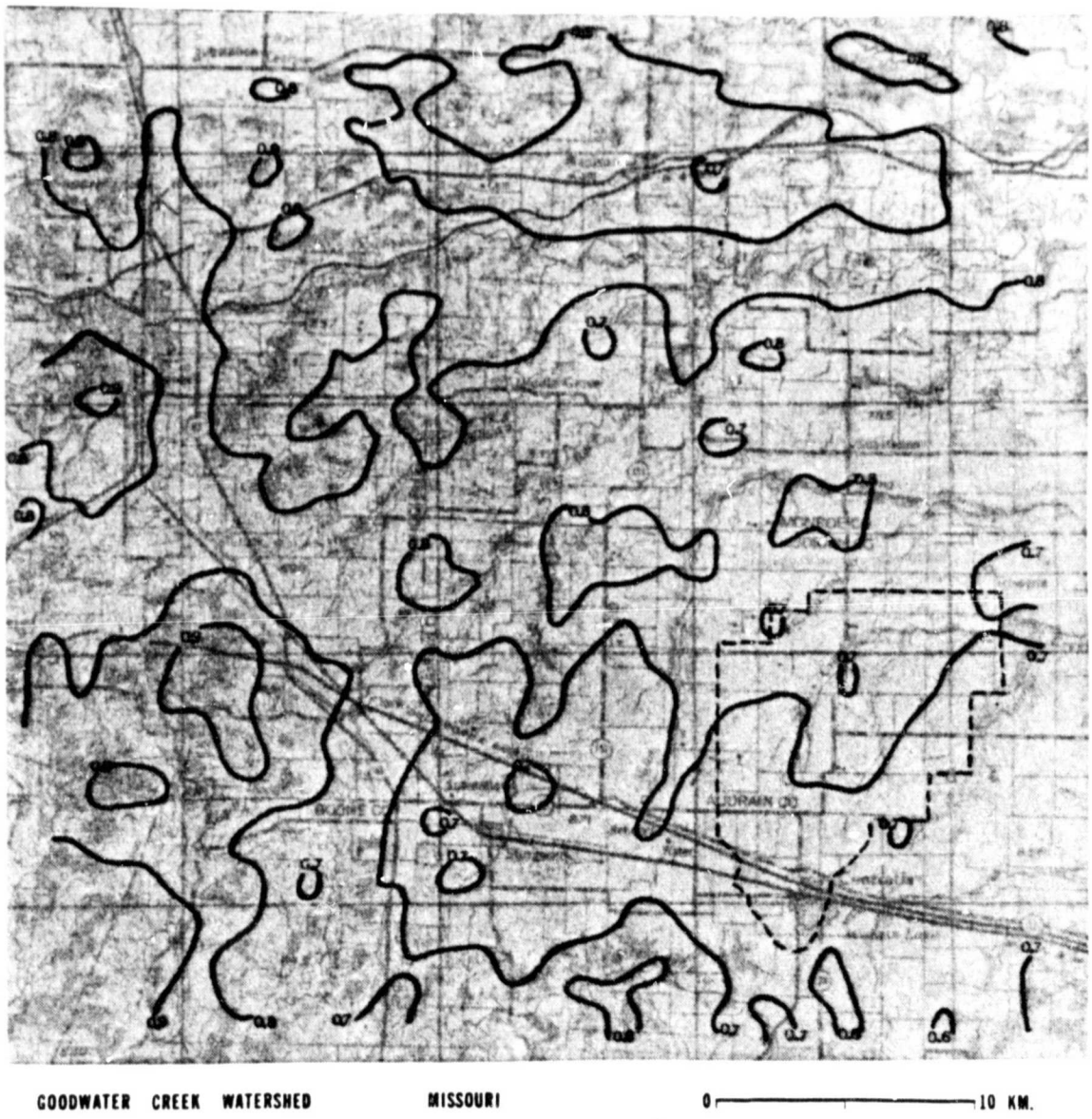

Figure 15. Moisture availability analysis, September 29, 1978

.70 and .85. Lowest values of M occur near Centralia, while values greater than .90 are observed mainly along the left edge of the figure, where forested land prevails. An inverse correlation between M and daytime temperatures is noted for this case, as well as for the previous case.

Relative maxima of M are observed along forested areas and several creeks, including Perche Creek, Silver Fork, Saling Creek, Salt River, a forested site west of Moberly and Sugar Creek Lake. In general, forested areas exhibit the highest values of M (.80 to 1.0). Creeks exhibit a range of .75 to .95 and agricultural sections show a variation of .60 to .80. Although Moberly and Centralia do not appear as well defined regions of moisture minima, they are located in broad regions of low M.

Figure 16 is an enlarged and unsmoothed analysis of moisture availability over the Goodwater Watershed (the dashed region). M varies from under .60 to greater than .90, with the wettest locations found over cropland. Features such as Saling Creek, Silver Fork and Long Branch Creek show up as relative moisture availability maxima. During June, the southern end of Long Branch Creek appears as a moisture minimum: here, it appears as a moisture maximum.

Within the watershed itself, M mainly varies from .60 to .75 with a remote maximum of .90 a kilometer or two east of Goodwater Creek. Figure 17 presents rainfall amounts for September 20, 1978 (the last rainfall measured prior to September 29). Heaviest rainfall occurred over the northern half of the watershed. Returning to the analysis of moisture availability (Figure 16), the northern half of the watershed has measured values of M greater than .70 while the south is represented

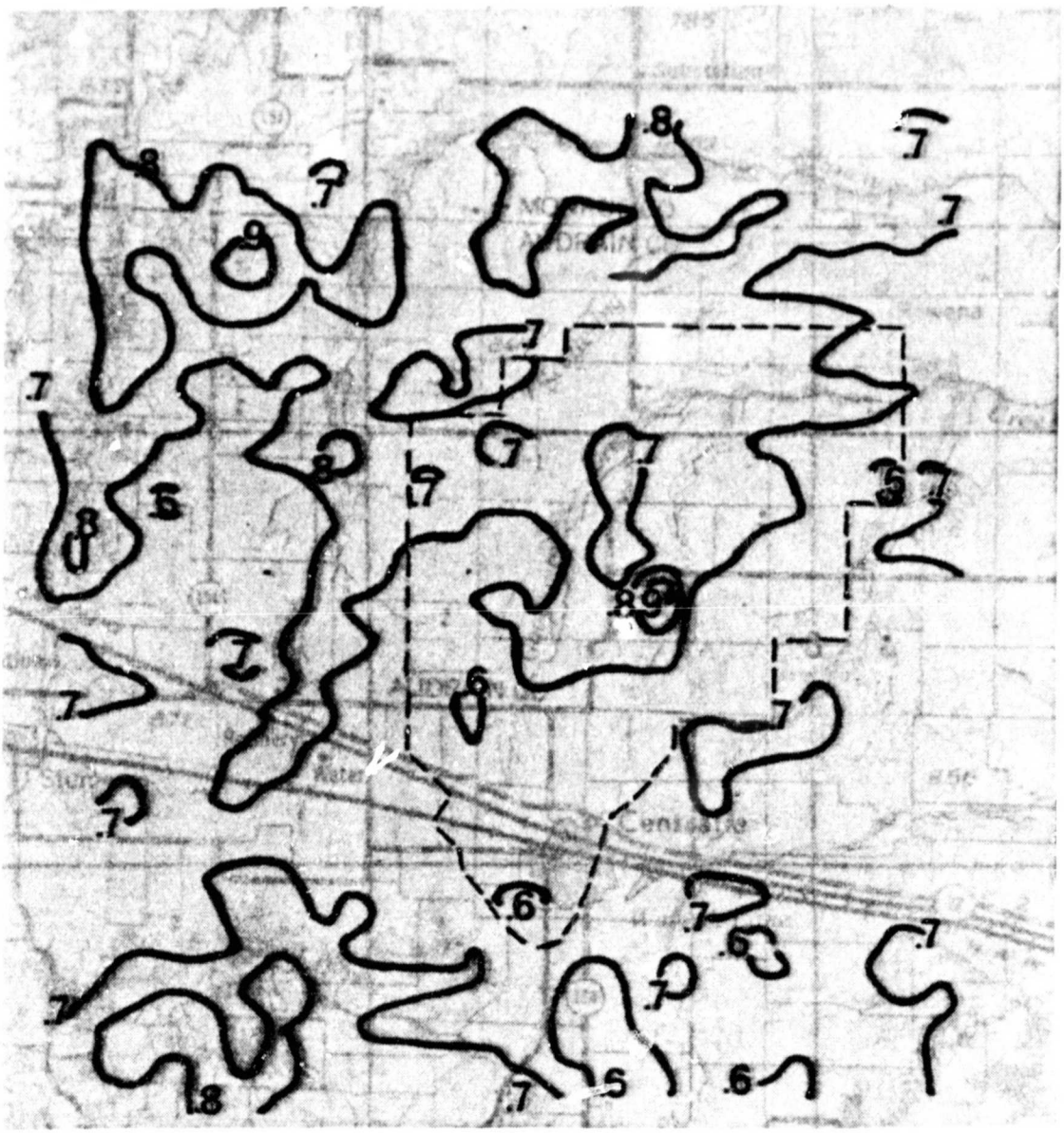

Figure 16. Enlargement of unsmoothed moisture availability analysis over the Goodwater Watershed (enclosed by dashed lines), September 29, 1978

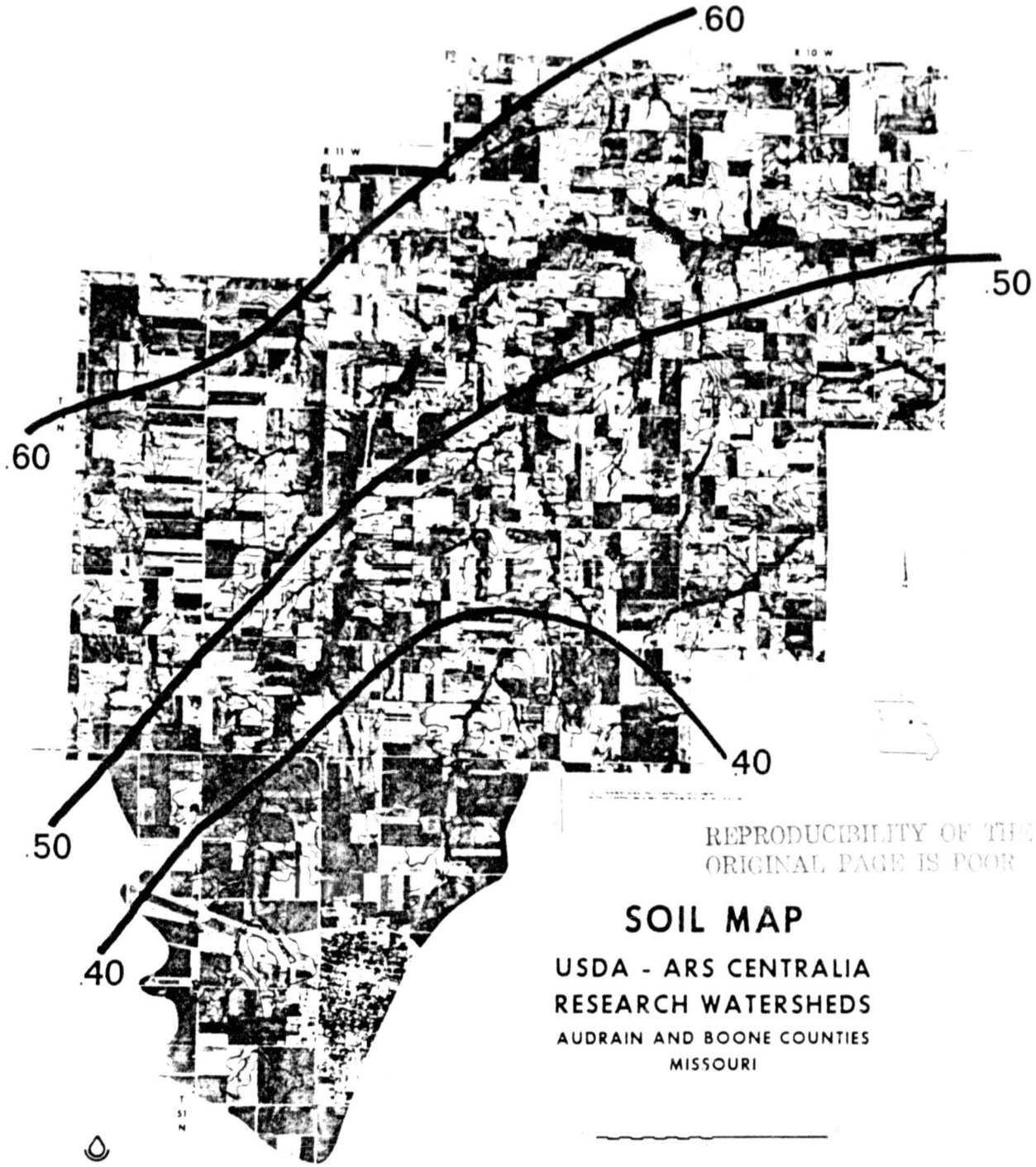

Figure 17. Rainfall amounts (in inches) over the Goodwater Watershed, September 20, 1978

by M values of less than .70. This difference can probably be attributed to local differences in rainfall amounts, which are distributed in a similar manner to M (Figure 17); higher amounts occurring in the northwest.

3.3.4 September 29 Surface Heat Flux, H_o

The surface heat flux analysis (Figure 18) was evaluated for the early afternoon of September 29. The isopleths resemble the daytime isotherm pattern, as was noted in the June case. The magnitudes of heat flux are considerably smaller on September 29 than those determined for the afternoon of June 10th, the former varying from approximately 80 Wm^{-2} to 170 Wm^{-2}. Smallest values are found near water bodies and forests. Highest values are observed over the daytime temperature maximum, south of Centralia.

Agricultural regions are represented by a heat flux variation of 80 Wm^{-2} to 170 Wm^{-2}, which represents the entire range observed within the figure. High values are found over areas with low moisture availability while the converse also holds true. Moberly and Centralia are depicted as localities with comparitively low heat flux, but Centralia has a much higher reading (160 Wm^{-2}) than Moberly (110 Wm^{-2}). The heat flux maximum (170 Wm^{-2}) located just south of Centralia corresponds to the location where maximum daytime temperatures and minimum moisture availability is observed. H_o varies from 125 Wm^{-2} to 160 Wm^{-2} over the (dashed) Goodwater Watershed.

3.4.5 September 29 Evaporative Flux, E_o

The surface evaporative flux, contoured in Figure 19, exhibits a range of 375 Wm^{-2} to 465 Wm^{-2}. As expected, evaporative fluxes

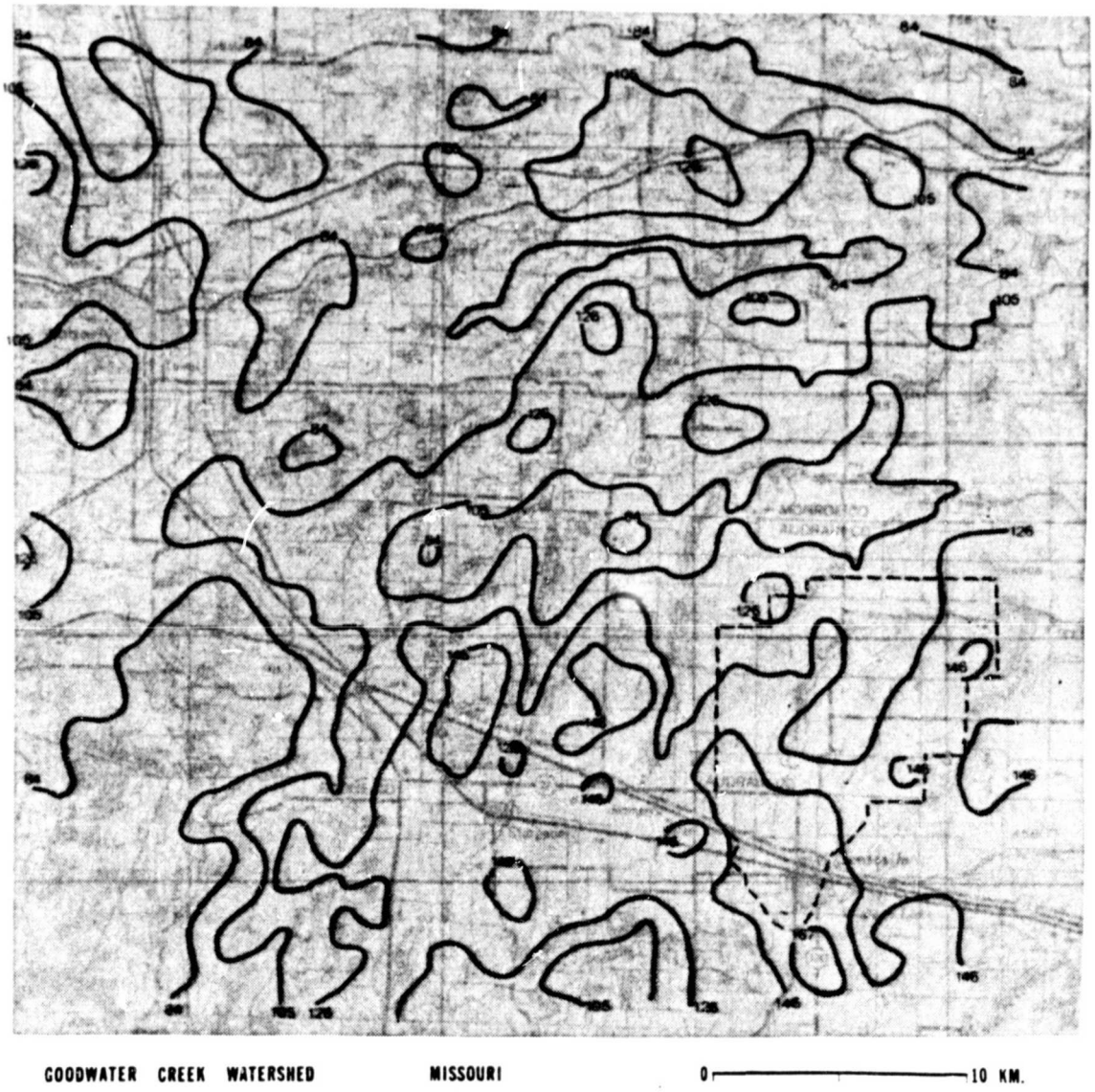

Figure 18. Sensible heat flux (Wm^{-2}) at approx. 2:00 p.m., September 29, 1978 (R_N = 550 Wm^{-2})

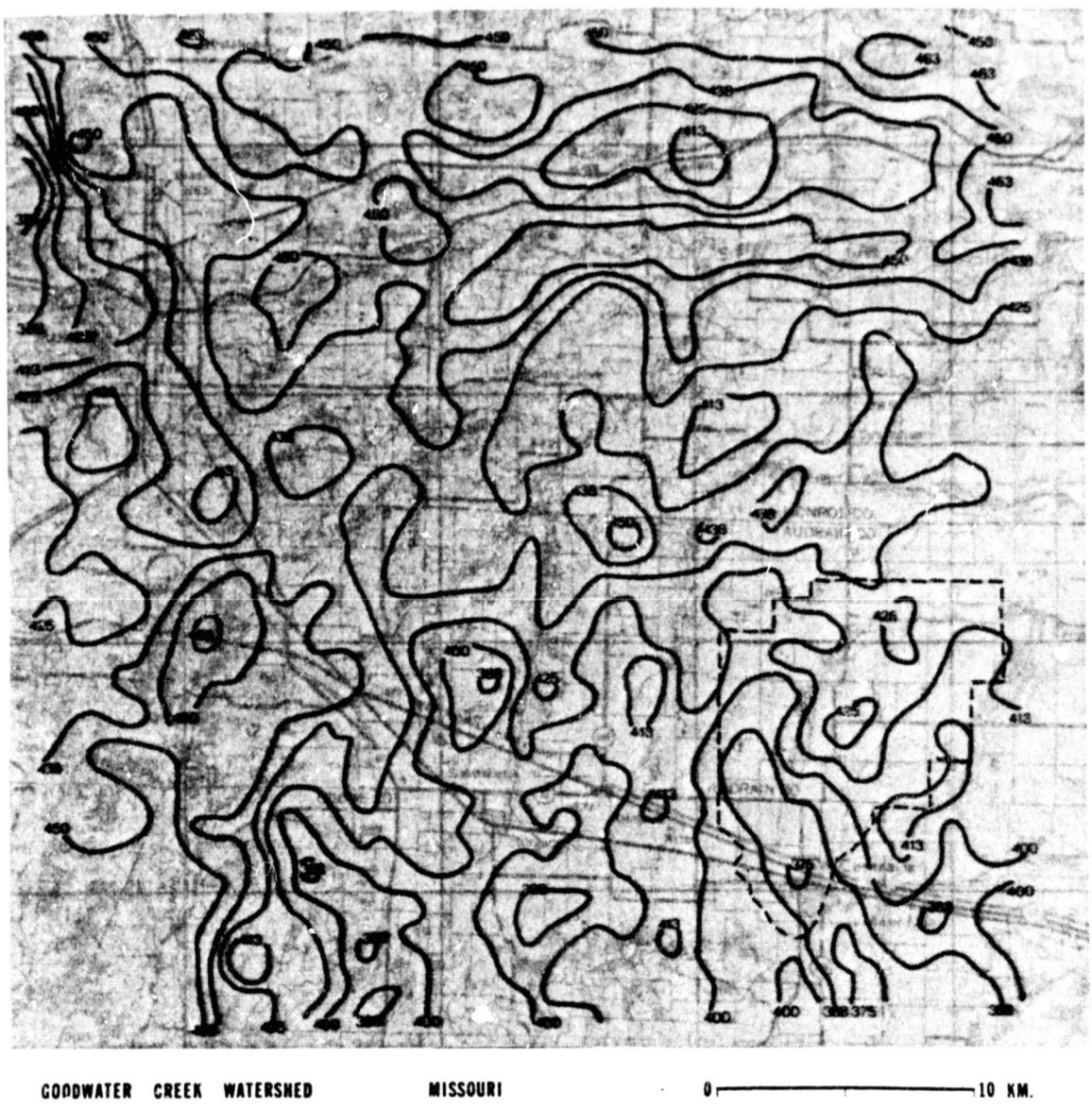

Figure 19. Evaporative flux (Wm^{-2}) at approx. 2:00 p.m., September 29, 1978 (R_N = 550 Wm^{-2})

are highest over forests and creeks, and variable over cropland. Magnitudes of moisture flux measured on September 29 are similar to those measured in June.

Sites with large evaporative fluxes, such as Sugar Creek Lake, forested regions near Perche Creek, Coon Creek, Elk Creek and the Salt River, also have high moisture availabilities. Most agricultural regions exhibit a range of 375 Wm^{-2} to 450 Wm^{-2}. Largest values are found approximately twelve kilometers south and eight kilometers north of Moberly and along the Salt River. Smallest values are found a few kilometers south of Centralia.

Over the Goodwater Watershed, E_o varies from 375 Wm^{-2} over Centralia to 425 Wm^{-2} in the northeast. A tongue of low values of evaporative flux extends up along the western edge of the dashed area.

3.4.6 September 29 Thermal Inertia, P

The analysis of thermal inertia, Figure 20, reveals a larger variation of P than was observed for the June study. Values range from .03 to .065, but most values vary between .03 and .05. The distribution of P closely corresponds to the nighttime temperature pattern. Large values of thermal inertia correspond to high nighttime temperatures and small values of thermal inertia to low nighttime temperatures.

Relatively high values of P (greater than .04) can be observed along the western and southern edges of the figure, which are locations dominated by forests and creeks. Relatively low values are noted over agricultural districts, where the diurnal range of temperature is the largest.

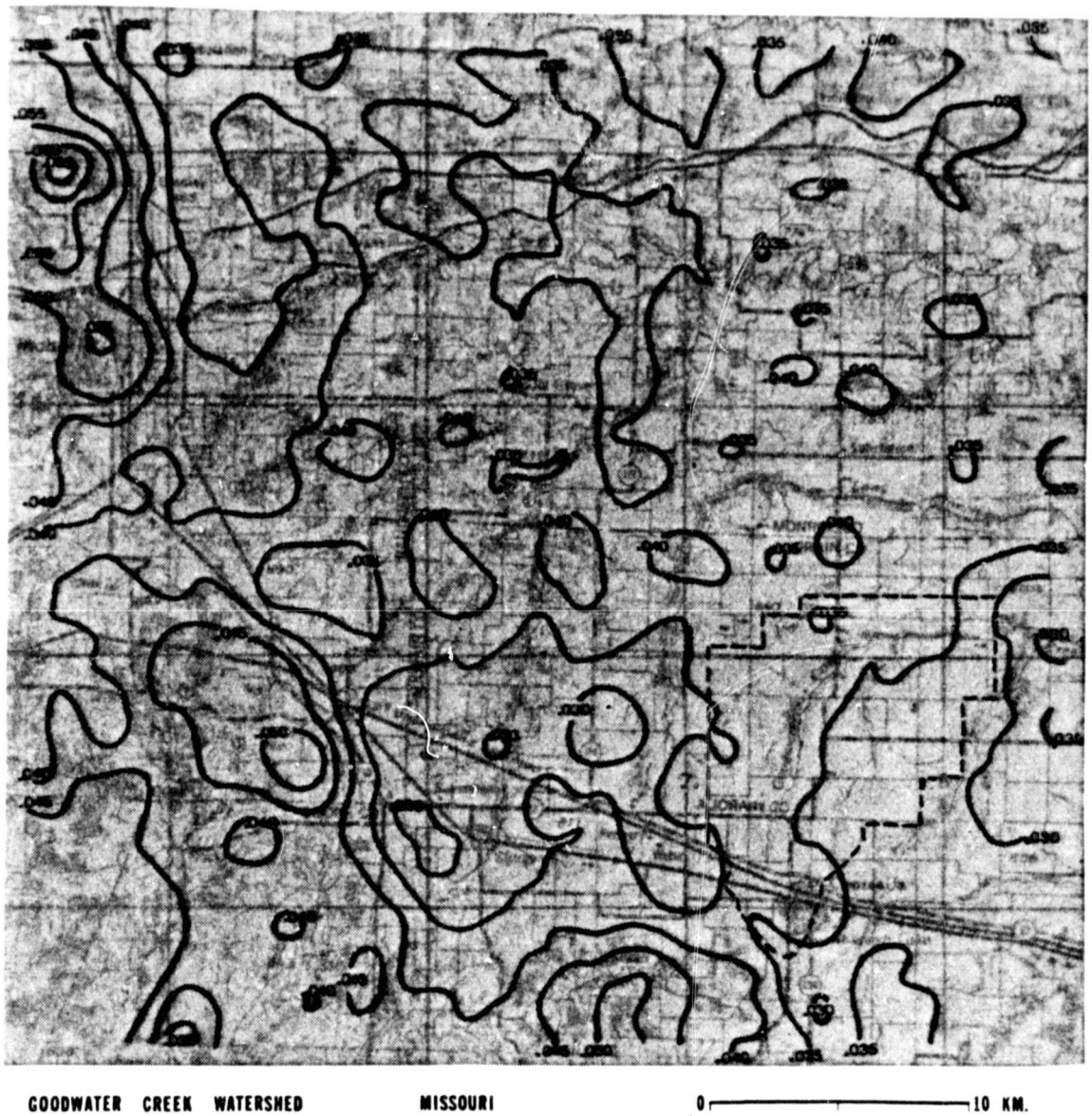

Figure 20. Thermal inertia analysis (cal cm^{-1} K^{-1} $sec^{-1/2}$), September 29, 1978

A thermal inertia maximum (.065) is once again observed over Sugar Creek Lake. Moberly is easily identified as a P maximum with a value of .055, while Centralia is weakly reflected by a bend in a contour (.035).

4.0 SUMMARY AND CONCLUSIONS

4.1 Summary of Results

Daytime temperatures on June 10, 1978 were generally higher than those of September 29, 1978. Across the Goodwater Watershed and surrounding countryside, temperatures varied mainly between 23°C and 29°C on June 10th, while on September 29th, surface temperatures were between 20°C and 24°C. Thus, a smaller range of temperatures is observed on the later date.

In both cases, the horizontal temperature variation across the region at night was less than that during the daytime hours. However, in comparison, a slightly larger range of nighttime temperatures was measured on September 29 (a variation between 3.5°C and 6.5°C) than on June 10 (a variation between 2.0°C and 6.0°C).

The amount of surface moisture over the Goodwater Watershed and surrounding countryside, as parameterized by M, was uniformly greater on September 29 than on June 10. Moisture availability M varied from under .40 to greater than .90 during June, and from about .60 to greater than .90 during the September case.

Although the magnitudes of evaporative flux measured in the fall case are similar to those measured in the spring case, the ratio of the moisture flux E_o to the net radiation R_N is larger in the later case than in the earlier one. On September 29th, when the surface moisture content was uniformly greater than in June, the moisture flux E_o was 70% to 80% of the net radiation (approximately 550 Wm^{-2}), while on June 10th, E_o was only 60% to 70% of the net radiation (approximately 650 Wm^{-2}). Thus, the wetter surface observed in September apparently

allows for a greater fraction of available radiant energy to be converted into latent heat flux.

Conversely, the averaged Bowen Ratio, the ratio of sensible heating to latent heating, was larger in June (.40) than in September (.30), since a dry surface suppresses evaporation and allows for a greater fraction of available radiant energy to be converted into sensible heating. On June 10th, sensible heating amounted to 15% to 30% of the net radiation, while on September 29th, it was only 10% to 20% of R_N.

Many specific surface features, such as forests and creeks, were reflected as distinct minima or maxima of moisture availability. Forested regions consistently appear as M maxima, exhibiting a range of 0.8 to 1.0. Creeks are represented by a larger variation of moisture availability from one to another. The dryness of some creeks suggests that drying or a reduction of vegetation has occurred. Moberly and Centralia are observed as moisture availability minima on June 10, but are not easily identifiable in late September analyses. Both towns are represented by M of .40 or less on June 10, but the two villages are represented by values greater than .60 on September 29.

Agricultural regions exhibited the greatest variation of surface moisture over the region for the two cases examined. M varied between .35 and .60 over cropland on June 10, while on September 29, M exhibits a range between .70 and .85. A difference in the vegetative cover of the soil surface is proposed as the reason behind the moisture variation, since the average rainfall over the area prior to each case is similar.

Detailed analyses of moisture availability over the Goodwater Watershed are presented in Figures 8 and 16. In both cases, moisture maxima and minima are related to regional features, such as creeks, forests, etc. Saling Creek and Silver Fork appear as moisture maxima while Centralia is located within contours of relatively low moisture availability. A surprising discrepancy between the two cases occurs over the southern section of Long Branch Creek, where M is a maximum (.80) on September 29, and a minimum (.40) on June 10, possibly due to a change in vegetation.

In both analyses of moisture availbaility, small elevations of M correspond to local maxima in rainfall accumulations.

4.2 Conclusions

Carlson and Boland's technique to infer the effective moisture availability by combining satellite data with a numerical simulation of the diurnal boundary layer temperature wave, provides a quantitative approach for examining spatial and temporal changes in the surface moisture availability. For the first time, a representation of moisture has been inferred remotely over a large region.

When related to specific regional features, such as forests and croplands, and to rainfall, the patterns and horizontal variations of moisture availability over an agricultural domain in Missouri appear reasonable. Over several locations, variations of moisture availability probably result from horizontal rainfall differences. Significant changes in the surface moisture availability between June 10, 1978 and September 29, 1978 have also been shown; the former being drier. Rainfall, alone, cannot account for the temporal

variations. Rather, the variation in the distribution of surface moisture availability must also be attributed to a change in the character of the vegetative canopy between late spring and early fall. Specifically, in late spring, the surface canopy probably consists of short vegetation stubble and bare soil, whereas in early autumn, fully developed plant canopies effectively become the "ground surface".

There are three problems which presently limit the applicability of this measurement technique. First, the examination of small scale surface features is dependent on the horizontal resolution of the satellite temperature measurements. At present, the Heat Capacity Mapping Mission (HCCM) provides the best spatial resolution in the infrared (.6 km) of any operational satellite, but data is infrequent, limiting the number of studies possible for a given location. Tiros-N offers more frequent observations, but its horizontal resolution is half that of HCCM. Secondly, this technique does not enable one to monitor surface moisture on a continuous basis because of interruptions in the periodic measurement schedule by cloudiness. Third, and finally, the processing and analysis of satellite data currently requires a substantial period of time, and therefore, real time analyses of case studies are infeasible.

In spite of these difficulties, it is now possible to assess the moisture content of many types of surfaces, including farmland, forests, flood plains and urban centers. Many more case studies are necessary to fully evaluate the utility of this measurement method.

The Carlson-Boland technique holds promise for a variety of

practical applications, such as those mentioned in Section 1.1. Future investigators should focus attention on the behavior of certain types of surfaces, in particular, farmlands and flood plains, where changes in the surface moisture can drastically affect man's essential activities. As an example, two analyses of the moisture availability over an agricultural region, one during an extended period of drought and the other following an excessively wet spell, can provide an interesting contrast of moisture conditions and perhaps shed some light on how the moisture availability changes with time.

Many applications to study insect and plant pest outbreaks, flooding, drought, erosion and landslide potential are foreseen, possibly with the use of the next scheduled ERTS satellite, which is to possess an infrared channel with a thirty meter spatial resolution at the ground.

REFERENCES

Augustine, J., 1978: A Detailed Analysis of Urban Ground Temperature and Albedo Using High Resolution Satellite Measurements. M. S. Thesis, Department of Meteorology, The Pennsylvania State University.

Bauer, A., Vasey, E. H., Young, R. A. and Ozbun, J. L., 1967: Stored soil moisture best guide to nitrogen needs. Farm Research, 24, 15-24.

Blackadar, A. K., 1976: Modeling the nocturnal boundary layer. Third Symp. on Atmospheric Turbulence, Diffusion, and Air Quality, Raleigh, N.C., 26-29, Oct. 19-22, 1976.

Blanchard, M. B., Greeley, R. and Goettelman, R., 1974: Use of visible, near-infrared, and thermal infrared remote sensing to study soil moisture. NASA Technical Memorandum. 9 p.

Boland, F. E., 1977: A Model for Determining Surface Temperatures and Sensible Heat Fluxes over the Urban-Rural Complex. M. S. Thesis, Department of Meteorology, The Pennsylvania State University.

Carlson, T. N. and Boland, F. E., 1978: Analysis of urban-rural canopy using a surface heat flux temperature model. J. Appl. Meteor., 17, 998-1013.

Cook, R. J. and Papendick, R. I., 1971: Effect of soil water on microbial growth, antagonism, and nutrient availability in relation to soil-borne fungal diseases of plants. In Root Diseases and Soil-Borne Pathogens. T. A. Toussoun, R. V. Bega, and P. E. Nelson, eds., Berkeley: Univ. Calif. Press, pp. 81-88.

Davies, J. A., and Allen, C. D., 1973: Equilibrium, potential and actual evaporation from cropped surfaces in Southern Ontario. J. Appl. Meteor., 12, 649-657.

Dodd, J. K., 1979: Determination of Surface Characteristics and Energy Budget Over an Urban-Rural Area Using Satellite Data and a Boundary Layer Model. M. S. Thesis, Department of Meteorology, The Pennsylvania State University.

Idso, S. B., Jackson, R. D. and Reginato, R. J., 1975: Detection of soil moisture by remote surveillance. American Scientist, 63, 549-557. a.

Idso, S. B., Jackson, R. D. and Reginato, R. J., 1975: Estimating evaporation: a technique adaptable to remote sensing. Science, 189, 991-992. b.

REFERENCES (Continued)

Idso, S. B., Jackson, R. D. and Reginato, R. J., 1976: Compensating for environmental variability in the thermal inertia approach to remote sensing of soil moisture. J. Appl. Meteor., 15, 811-817.

Idso, S. B., Jackson, R. D. and Reginato, R. J., 1977: Remote sensing of crop yields. Science, 196, 19-25.

Idso, S. B., Jackson, R. D., Reginato, R. J., Kimball, B. A. and Nakayama, F. S., 1975: The dependence of bare soil albedo on soil water content. J. Appl. Meteor., 14, 109-113. c.

Idso, S. B., Reginato, R. J. and Jackson, R. D., 1977: An equation for evaporation from soil, water, and crop surfaces adaptable to use by remote sensing. Geophys. Res. Letters, 4, 187-188.

Idso, S. B., Schmugge, T. J., Jackson, R. D. and Reginato, R. J., 1975: The utility of surface temperature measurements for the remote sensing of surface soil water status. J. Geophys. Res., 80, 3044-3049. d.

Jackson, R. D., 1973: Diurnal changes in soil water content during drying. In Field Soil Water Regime. Soil Science Society of America, pp. 37-65.

Myers, V. J. and Neilman, M. D., 1969: Thermal infrared for soil temperature studies. Photogrammetric Engrg., 10, 1024-1032.

Nappo, C. J., 1975: Parameterization of surface moisture and evaporation rate in a planetary boundary layer model. J. Appl. Meteor., 14, 289-296.

Reginato, R. J., Idso, S. B., Vedder, J. F., Jackson, R. D., Blanchard, M. B. and Goettelman, R., 1976: Soil water content and evaporation determined from ground-based and remote measurements. J. Geophys. Res., 81, 1617-1620.

Rose, C. W., 1968: Water transport in soil with a daily temperature wave. Aust. J. Soil Res., 6, 31-57.

Schmugge, T., Gloersen, P., Wilheit, T. and Geiger, F., 1974: Remote sensing of soil moisture with microwave radiometers. J. Geophys. Res., 79, 317-323.

Tanner, C. B. and Pelton, W. G., 1960: Potential evapotianspiration estimates by the approximate energy balance method of Penman. J. Geophys. Res., 65, 3391-3412.

Tennekes, H., 1973: A model for the dynamics of the inversion above a convective boundary layer. J. Atmos. Sci., 30, 558-567.